

1   **Running head:** Pilot whale PCoD model

2

3   **Bio-energetic modeling of medium-sized cetaceans shows high sensitivity to**  
4   **disturbance in seasons of low resource supply**

5

6   **Vincent Hin** (corresponding author). Institute for Biodiversity and Ecosystem Dynamics,  
7   University of Amsterdam, Amsterdam, The Netherlands; [V.Hin@uva.nl](mailto:V.Hin@uva.nl)

8   **John Harwood.** Centre for Research into Ecological and Environmental Modelling, University  
9   of St Andrews, St Andrews, UK; [jh17@st-andrews.ac.uk](mailto:jh17@st-andrews.ac.uk)

10   **André M. de Roos.** Institute for Biodiversity and Ecosystem Dynamics, University of  
11   Amsterdam, Amsterdam, The Netherlands; [A.M.deRoos@uva.nl](mailto:A.M.deRoos@uva.nl)

12

13   **Abstract**

14   Understanding the full scope of human impact on wildlife populations requires a framework to  
15   assess the population-level repercussions of nonlethal disturbance. The Population Consequences  
16   of Disturbance (PCoD) framework provides such an approach, by linking the effects of  
17   disturbance on the behavior and physiology of individuals to their population-level  
18   consequences. Bio-energetic models have been used as implementations of PCoD, as these  
19   integrate the behavioral and physiological state of an individual with the state of the  
20   environment, to mediate between disturbance and biological significant changes in vital rates  
21   (survival, growth and reproduction). To assess which levels of disturbance lead to adverse effects  
22   on population growth rate, requires a bio-energetic model that covers the complete life cycle of  
23   the organism under study. In a density-independent setting, the expected lifetime reproductive

24 output of a single female can then be used to predict the level of disturbance that leads to  
25 population decline. Here, we present such a model for a medium-sized cetacean, the long-finned  
26 pilot whale (*Globicephala melas*). Disturbance is modeled as a yearly recurrent period of no  
27 resource feeding for the pilot whale female and her calf. Short periods of disturbance lead to the  
28 pre-weaned death of the first one or more calves of the young female. Higher disturbance levels  
29 also affect survival of calves produced later in the life of the female, in addition to degrading  
30 female survival. The level of disturbance that leads to a negative population growth rate strongly  
31 depends on the available resources in the environment. In seasonal environments, this has  
32 important repercussion for the timing of disturbance. The duration of disturbance that leads to a  
33 negative population growth rate is on average 3 times higher when disturbance happens during  
34 seasons of high resource availability, in contrast to disturbance happening during seasons of low  
35 resource supply. Although our model is specifically parameterized for pilot whales, it provides  
36 useful insights into the general consequences of nonlethal disturbance. If appropriate data on life  
37 history and energetics are available, it can be used to provide management advice for specific  
38 species or populations.

39 **Key-words:** *Globicephala melas*, population consequences of disturbance, marine mammals,  
40 Dynamic Energy Budget model, life history

41

## 42 **Introduction**

43 The increase of human activity in the marine environment has led to concern about the effects of  
44 disturbance on marine mammals (Halpern et al. 2008, DeRuiter et al. 2013, Maxwell et al. 2013,  
45 Fleishman et al. 2016, Parsons 2017). Several sources of disturbance (ship traffic, seismic  
46 surveys, use of military sonar) can lead to a variety of responses and impacts on marine

47 mammals, such as decrease/cessation of feeding, avoidance behavior, temporary and permanent  
48 effects on hearing, and death (National Research Council 2003). Especially the link between the  
49 use of military sonar and the strandings of whales and dolphins has received considerable  
50 attention (Cox et al. 2006, Parsons et al. 2008, Tyack et al. 2011, Parsons 2017). While the link  
51 between disturbance and its (short term) effect on behavior, feeding, and health of individuals is  
52 becoming more apparent (Sivle et al. 2012, Miller 2012, DeRuiter et al. 2013, Christiansen and  
53 Lusseau 2015, Friedlaender et al. 2016), assessing the (long-term) population consequences is  
54 challenging and involves many uncertainties. These arise from (among others) the inaccessibility  
55 of the marine environment and the species in question, uncertainty about many life-history  
56 parameters and processes, the difference in timescale between a disturbance event and its  
57 consequences for populations, and the lack of information about behavioral responses that might  
58 aggravate or compensate the effect of a disturbance (Harwood and Stokes 2003, National  
59 Research Council 2005).

60 The PCoD (population consequences of disturbance) framework is a conceptual model to  
61 connect disturbance to its population-level consequences by means of a number of transfer  
62 functions (New et al. 2014, Harwood et al. 2016, Pirotta et al. 2018a). These transfer functions  
63 sequentially link the properties of disturbance to behavioral changes, life history functions, vital  
64 rates and population effects. Although the precise nature of many of these transfer functions is  
65 unknown, it is likely that they are highly context-dependent (National Research Council 2005,  
66 Friedlaender et al. 2016). For example, disturbance will have a different effect on lactating  
67 females in a resource-poor environment than on non-lactating females in a resource-rich  
68 environment. This context-dependency calls for an approach that includes the state of an  
69 individual (e.g. energy reserve, reproductive status) and the state of the environment (e.g.

70 resource density, presence of predators) to mediate between disturbance and biologically  
71 significant changes in vital rates. Bio-energetic models represent such an approach and have  
72 been used to assess the population consequences of disturbance for a variety of marine mammal  
73 species (New et al. 2013, Villegas-Amtmann et al. 2015, Costa et al. 2016, McHuron et al. 2016,  
74 Pirotta et al. 2018b). However, the amount and quality of data needed to parameterize and  
75 validate such models are unavailable for many species (Harwood et al. 2016).

76 Bio-energetic models that assess the effect of disturbance on marine mammals focus on  
77 female life history and, in most cases, only take into account a single reproductive cycle  
78 (Braithwaite et al. 2015, Christiansen and Lusseau 2015, Villegas-Amtmann et al. 2015,  
79 McHuron et al. 2016, Pirotta et al. 2018b). From an energetics perspective, the reproductive  
80 period, and especially lactation, is the most demanding part of female life history and also of  
81 considerable importance for population growth. However, in order to assess under which  
82 conditions disturbance leads to negative population growth rates, it is necessary to model female  
83 life history and energetics across the entire life (McHuron et al. 2018, Pirotta et al. 2018a). In the  
84 absence of any density-dependence, population decline will occur if the expected lifetime  
85 reproductive output of a single female ( $R_0$ ) is smaller than 1 (counting females only) (Caswell  
86 2001). Provided that male density does not influence pregnancy rates of females, accounting for  
87 males only becomes important in the presence of density-dependence. Therefore, it is possible to  
88 gain insight about the population consequences of disturbance in the absence of density-  
89 dependence by simply looking at the expected lifetime reproductive output of a single female.

90 Here we present a generic bio-energetic model for a marine mammal life history to assess  
91 the population consequences of disturbance and its dependence on environmental resource  
92 availability. The model describes the entire life of a female individual. In addition, we follow

93 calf survival and development until weaning. Although the structure of the model is general  
94 enough to describe the life history of any (marine) mammal species, we parameterize and tailor  
95 this model for long-finned pilot whales (*Globicephala melas*), a medium-sized cetacean in which  
96 long-distance migration is absent and feeding occurs continuously throughout the year. The  
97 choice of this species is motivated by the relatively rich amount of data on pilot whale bio-  
98 energetics and life history processes (The International Whaling Commission 1993) and the  
99 availability of observations on the response of this species to (sound) disturbance (Wang and  
100 Yang 2006, Dolman et al. 2010, Sivle et al. 2012, Miller 2012, Wensveen et al. 2015, Isojunno et  
101 al. 2017). When sufficient data are available, the model could be easily parameterized for other  
102 species, including species that make long-distance migrations with interrupted feeding (e.g.  
103 Villegas-Amtmann et al. 2015). With this model, we aim to understand how disturbance affects  
104 reproductive abilities of the female and survival of the female and her calves, as integrated in the  
105 expected lifetime reproductive output. We assess the consequences of a yearly recurrent  
106 disturbance period that can vary in duration and timing of onset within the year. The model  
107 assumes that individual pilot whales (both the female and her calves) can behaviorally  
108 compensate for disturbance by an increase in feeding effort when body condition decreases and  
109 sufficient resources are available. We show how a number of life-history characteristics change  
110 with increasing disturbance intensity. Furthermore, we outline how the effect of disturbance  
111 depends on environmental resource availability and its seasonal variation.

112

### 113 **Model Formulation**

114 Because the life history processes of the female and her calves (growth, reproduction and  
115 survival) depend on energy we use a Dynamic Energy Budget (DEB) model to specify how

116 assimilated energy is allocated to different processes (Figure 1; Lockyer 2007, Kooijman 2010,  
117 Lika and Kooijman 2011). Energy can temporarily be stored in a ‘reserve compartment’, which  
118 functions as a buffer for incoming and outgoing energy flows (De Roos et al. 2009). This reserve  
119 compartment is quantified by reserve mass and represents primarily fat tissue that is mainly  
120 stored internally (in and around visceral organs and muscle tissue), but also in blubber of pilot  
121 whales (Lockyer 1993, 2007). Reserve mass can be mobilized to serve energetic needs and  
122 controls various life history functions (Lockyer 2007, Miller et al. 2011). It therefore links the  
123 effects of disturbance and environmental conditions to survival and reproduction and, ultimately,  
124 population dynamics. To control for differences in absolute size during ontogeny, we use relative  
125 reserve mass (reserve mass over total body mass, also referred to as ‘body condition’) as a  
126 measure of individual health. A good body condition is required to successfully raise a calf  
127 (pregnancy and lactation) and a poor body condition compromises survival and decreases life  
128 expectancy. The joint outcome of survival and reproduction is summarized by the expected  
129 lifetime reproductive output ( $R_0$ ) of the female. More precisely,  $R_0$  is defined as the expected  
130 number of weaned calves that a single female will produce from weaning age onwards. Age at  
131 weaning, instead of age at birth, was chosen as a starting point for the calculation of  $R_0$ , because  
132 mammalian individuals only become independent from their mother at weaning. We therefore  
133 simulate the life history of the female from weaning age onwards and, when lactating, we  
134 simultaneously track the life history of the calf. A description of the model’s most important  
135 features is outlined below and summarized in Table 1. Full model details and parameters are  
136 presented in the Appendix S1.

137

138 *Bio-energetics*

139 The DEB model that specifies the allocation of energy is taken from De Roos et al. (2009) and a  
140 schematic overview of the energy allocation scheme is shown in Figure 1. Energy is derived  
141 from the environment through resource feeding and, in addition, calves derive energy from the  
142 female through lactation. Energy is expended on field and maintenance metabolism, growth  
143 costs, gestation costs (when pregnant) and lactation costs (when lactating). All rates of energy  
144 flow (connecting lines in Figure 1) depend on the state of the environment and the state of the  
145 individual. The environment state is captured by resource density ( $R$ ), while the individual state  
146 consists of age ( $a$ , days), structural size (length  $l$ , in cm, and mass  $S$ , in kg), reserve mass ( $F$ , in  
147 kg) and reproductive status (see Table 1 for all individual state-variables and associated  
148 parameters). The structural component of an individual includes all tissue that cannot be used to  
149 fuel growth and metabolic costs, lactation or gestation, such as bones and vital organs (Kooijman  
150 2010). In contrast, assimilated energy or energy mobilized from the reserve compartment is used  
151 for such purposes. Structural mass changes due to structural growth. Dynamics of reserve mass  
152 are given by the difference between total energy assimilation and total energy expenditure (see  
153 below).

154

155 *Structural growth*

156 Growth in structural mass of mammals is best represented by a demand type of growth, in which  
157 structural growth rate and asymptotic structural mass do not vary with the rate of assimilated  
158 energy. Instead, structural growth poses a certain energy demand on the environment. Based on  
159 pilot whale data in Bloch *et al.* (1993), we use a Von Bertalanffy length-age relationship  $l(a)$  for  
160 free-living individuals, with length at birth  $l_b = 177$ , asymptotic length  $l_\infty = 450$  and Von  
161 Bertalanffy growth rate  $k = 0.00045$  (Table 1, Appendix S1). The length-age relationship of a

162 fetus ( $l_p(\tau_p)$ ) is a linear function of time since conception,  $\tau_p$ , such that fetuses reach length at  
163 birth ( $l_b$ ) when the gestation period ( $T_p$ ) is due. Length is converted to structural mass ( $S$ ) by a  
164 power function (Bloch et al. 1993). Total body mass,  $W$ , equals the sum of structural mass  $S$  and  
165 reserve mass  $F$ . For pregnant females, total body mass also includes the structural mass of the  
166 fetus  $S(l_p(\tau_p))$ . Body condition, or relative reserve mass is defined as  $F/W$ .

167

168 *Resource feeding*

169 Resource assimilation rate scales with structural surface-area ( $S^{2/3}$ ; Kooijman 2010) and  
170 increases linearly with resource density  $R$ . The assumption of a linear functional response is  
171 based on the proposition that time spent on resource handling and/or digestion rarely limits  
172 resource intake rate. This assumption seems appropriate for pilot whales, which make short dives  
173 to find their food and spend most of their time at the surface (Heide-Jorgensen et al. 2002, Baird  
174 et al. 2002, Isojunno et al. 2017). Resource density is measured in assimilated energy per unit  
175 volume ( $\text{MJ} \cdot \text{m}^{-3}$ ) and therefore includes assimilation and conversion efficiencies of prey items  
176 by pilot whale individuals. The resource ingestion rate is furthermore proportional to an  
177 individual's feeding effort, which operates as a negative feedback of body condition on resource  
178 intake to ensure that the reserve mass does not grow out of bounds under favorable conditions  
179 (high resource availability or low energy expenditure). Similarly, the increase in feeding effort  
180 when body condition is low can be seen as a behavioral compensation response to disturbance or  
181 low resource availability. The feeding effort (0 – 1) is implemented as a decreasing sigmoidal  
182 function of body condition that equals 0.5 at the target body condition (parameter  $\rho$ ). Lockyer  
183 (1993) notes that body condition of pilot whales is independent of age and reproductive status  
184 and finds no evidence for an energy storage strategy to fulfil energetic demands of reproduction.

185 Consequently, we use a constant target body condition of 0.30 (Appendix S1). Finally,  
186 independent resource feeding depends on age in order to simulate the observation that young  
187 individuals are inexperienced resource foragers and that foraging skills increase with age  
188 (Lockyer 2007, Isojunno et al. 2017).

189

190 *Milk consumption*

191 In addition to resource feeding, calves gain energy through milk consumption with rate  
192  $I_L(a, S, F, W, F_m, W_m)$ . Like resource feeding, milk consumption scales with a two-thirds power  
193 of structural mass of the calf ( $S^{2/3}$ ), and is furthermore proportional to the lactation scalar  $\phi_L$ .  
194 Milk suckling decreases with increasing body condition of the calf in the same way as resource  
195 intake decreases with body condition. The mother also regulates milk provisioning in a manner  
196 that depends on her own body condition ( $F_m/W_m$ ). When the mother's body condition declines,  
197 milk provisioning is decreased and when her body condition reaches the starvation threshold  $\rho_s$ ,  
198 the mother ceases milk supply altogether. Finally, milk consumption depends on calf age.  
199 Beyond the first year of lactation, milk consumption decreases such that it becomes zero at the  
200 age of weaning,  $T_L$ . At  $T_L$  the calf becomes independent of the focal female and is no longer  
201 tracked during simulations. At any time before  $T_L$ , the milk supply will be interrupted only when  
202 the mother's body condition falls below  $\rho_s$ . The possibility of early weaning resulting from good  
203 body condition of mother and calf is not modeled. However, due to the dependence on female  
204 and calf body condition, milk consumption will be limited under these circumstances. Based on  
205 data in Martin and Rothery (1993) we adopt  $T_L = 1223$ . The parameters  $\phi_L$  and  $\rho_s$  were derived  
206 to be 2.7 and 0.15, respectively (see Appendix S1).

207

208    *Energetic costs*

209    Energetic costs are comprised of:  $C_M(W_M)$  - field metabolic costs depending on the maintenance  
210    body mass ( $W_M$ );  $C_G(S)$  - costs of growth in structural size;  $C_P(\tau_p)$  - pregnancy costs depending  
211    upon time since fertilization; and  $C_L(F, W, a_c, S_c, F_c, W_c)$  - lactation costs depending upon both  
212    age and body condition of the calf (subscript  $c$  indicates a calf variable), in addition to the body  
213    condition of the mother. Field metabolic costs include metabolic costs of maintenance and daily  
214    routine activity. Since maintenance of one kg of reserve mass is lower than that of one kg of  
215    structural mass, we introduce the maintenance body mass  $W_M$ . This measure uses the  
216    proportionality constant  $\theta_F$  to discount the contribution of reserve mass to maintenance costs  
217    (see Table 1) and is set to 0.2. Field metabolic costs are a  $\sigma_M$ -multiple of the maintenance mass,  
218    raised to the  $\frac{3}{4}$  power following Kleiber (1975). Somatic growth costs are equal to the derivative  
219    of the Von Bertalanffy growth function in structural mass, with proportionality constant  $\sigma_G$ . The  
220    same holds for pregnancy costs, which are equal to the derivative of fetal structural growth times  
221     $\sigma_G$ . Lactation costs equal the milk provisioning rate  $I_L$ , corrected by the conversion factor  $\sigma_L =$   
222    0.86, which accounts for efficiency of milk production (by the mother) and milk assimilation (by  
223    the calf) based on data from Lockyer (1993).

224

225    *Reserve dynamics*

226    Dynamics of reserve mass follow from adding and subtracting anabolic and catabolic processes  
227    and accounting for the conversion efficiency of catabolism and anabolism. Independent of  
228    individual status, reserve mass increases due to resource assimilation and decreases with field  
229    metabolic costs and somatic growth costs. For calves, milk suckling, in addition to resource  
230    feeding, increases reserve mass. For pregnant and lactating females, reserve mass also decreases

231 through gestation and lactation costs, respectively. The conversion efficiency ( $\varepsilon_i$ ) equals  $\varepsilon^+$  if  
 232 reserve dynamics are anabolic ( $dF/da > 0$ ) and  $\varepsilon^-$  if reserve dynamics are catabolic ( $dF/da <$   
 233 0). Reserve dynamics are described by:

$$\frac{dF}{da} = \begin{cases} \varepsilon_i^{-1}(I_R(a, R, S, F, W) + I_L(a, S, F, W, F_m, W_m) - C_G(l) - C_M(W_M)) & \text{Calves} \\ \varepsilon_i^{-1}(I_R(a, R, S, F, W) - C_G(l) - C_M(W_M) - C_P(\tau_c)) & \text{Pregnant female} \\ \varepsilon_i^{-1}(I_R(a, R, S, F, W) - C_G(l) - C_M(W_M) - C_L(F, W, a_c, S_c, F_c, W_c)) & \text{Lactating female} \\ \varepsilon_i^{-1}(I_R(a, R, S, F, W) - C_G(l) - C_M(W_M)) & \text{Other} \end{cases} \quad (1)$$

234

235 *Survival and life expectancy*

236 In order to calculate lifetime reproductive output, we track survival probabilities of the female  
 237 and her calves. There are two sources of mortality that decrease survival probability: age-  
 238 dependent mortality and starvation-induced mortality. Age-dependent mortality applies to all  
 239 individuals and consists of *i*) juvenile mortality that decreases with age, *ii*) senescence mortality  
 240 that increases with age and *iii*) background mortality that is constant with age (Barlow and  
 241 Boveng 1991, Bloch et al. 1993). Starvation-induced mortality is only applied when the body  
 242 condition of an individual falls below the starvation threshold ( $\rho_s$ ). Starvation mortality increases  
 243 with declining body condition according to a hyperbolic function, with the speed of increase  
 244 controlled by parameter  $\mu_s$  (De Roos et al. 2009).

245 Depending on the purpose of the simulation, life expectancy is either fixed or determined  
 246 randomly. A fixed life expectancy is used when illustrating the consequences of disturbance  
 247 across the entire life of the focal female. In this case, a life expectancy at birth of 60 years is used  
 248 (Bloch et al. 1993, Lockyer 2007). When only applying the age-dependent mortality as described  
 249 above, this corresponds to a survival threshold of  $2.266 \cdot 10^{-7}$ . Therefore, the female is  
 250 considered dead when her survival probability falls below this threshold. Because the female is  
 251 initiated at weaning, instead of at birth, she will reach the starvation threshold at an age that

252 slightly exceeds 60 years, in absence of starvation mortality. However, when survival is also  
253 decreased by starvation mortality, the female's life expectancy is decreased since she will cross  
254 the survival threshold at a younger age. The threshold survival probability of  $2.266 \cdot 10^{-7}$  is also  
255 used for calves, which implies that calves will only die before they reach weaning age in case of  
256 a substantial amount of starvation mortality.

257 A randomly determined life expectancy is used when calculating the expected lifetime  
258 reproductive output ( $R_0$ ) of the focal female. The calculation of  $R_0$  requires using the mean life  
259 expectancy of a female, in contrast to a fixed life expectancy of 60 years. Besides this, the  
260 random event of a calf death introduces variation in the timing of the next reproduction, which  
261 essentially creates an infinite number of possible life histories for the female. An accurate  
262 estimate of  $R_0$  requires averaging female reproductive output over all those possible life histories,  
263 or at least over a substantial subset. The randomly determined life expectancy is implemented by  
264 assigning a random number between zero and one to the female at weaning age and to each calf  
265 at birth. Subsequently, the individual (either the female or her calf) dies when its survival  
266 probability falls below this threshold value (De Roos et al. 2009). Both  $R_0$  and mean life  
267 expectancy can then be calculated by averaging the reproductive output and age at death of a  
268 sufficiently large number of life history simulations. For both random and fixed life  
269 expectancies, an individual also dies when its body condition falls below 0.005.

270

271 *Reproduction*

272 Reproduction is initiated when female reserve mass crosses the pregnancy threshold. This  
273 threshold is equal to the female reserve mass required to produce a neonate ( $F_{neonate}$ ), on top of  
274 the reserve mass that the female needs to offset starvation ( $\rho_s W$ ). The quantity  $F_{neonate}$  is

275 composed of *i*) the amount of female reserve mass required to produce the structural mass of a  
276 neonate and *ii*) the amount of female reserve mass transferred at birth from the mother to the  
277 neonate. Fetuses are assumed to grow in structural mass only and at birth they receive an amount  
278 of reserves that equals the starvation level threshold for neonates ( $\rho_s W_b$ ).

279 A non-pregnant and non-lactating female is assigned to the ‘resting’ state if her reserve  
280 mass is below the pregnancy threshold. When the reserve mass of the female crosses the  
281 threshold (*i.e.*  $F > \rho_s W + F_{neonate}$ ) she is assigned the ‘waiting’ state, as she does not become  
282 pregnant immediately. Instead, she awaits implantation. The waiting period ( $T_D$ ) lasts 445 days,  
283 which is based on the assumption of one ovulation per year and a chance of successful  
284 insemination of 0.82 (see Appendix S1). Pregnancy starts when the waiting period is due,  
285 irrespective of the reserve mass at that point in time. Pregnancy lasts for  $T_P = 365$  days.  
286 Lactation is initiated after the birth of the calf and lasts  $T_L = 1223$  days, unless the calf dies, or  
287 the mother stops milk provisioning due to poor body condition. A lactating female can reinitiate  
288 pregnancy (enter the waiting period) if her reserve mass is above the pregnancy threshold, but  
289 only when she is within the final  $T_P$  days of the lactation period. This additional condition  
290 prevents the occurrence of two calves that simultaneously feed from the mother. Taken together,  
291 the female will be in one of the following reproductive classes: resting, waiting, pregnant,  
292 lactating, and simultaneously waiting and lactating. In principle, the female could also be  
293 pregnant and lactating simultaneously, although the fact that the waiting period is longer than the  
294 gestation period ( $T_D > T_P$ ) prevents this from happening. The shortest possible interval between  
295 a weaning event and the next onset of pregnancy is hence  $445 - 364 = 81$  days. Given that the  
296 calf survives until the end of the lactation period, the shortest possible interval between two birth  
297 events (the inter-birth interval) is 4.57 years ( $81 + 365 + 1223$  days).

298

299 *Resource dynamics and disturbance*

300 Environmental resource density  $R$  fluctuates around a yearly mean value  $\bar{R}$  with a seasonal  
301 pattern (period is 365 days) and a relative amplitude of  $A$  ( $0 - 1$ ) (Table 1). With seasonal  
302 variation ( $A > 0$ ), resource density is at its mean value  $\bar{R}$  and increasing on the first day of each  
303 year ( $t = 0, 365$ , etc.), which we arbitrary label as the middle of spring. Since the simulation  
304 starts at  $t = 0$ , the simulated life of the female is therefore initiated in the middle of spring. With  
305 seasonal variation, the resource density peaks at  $t = 91$  days, which we call the middle of  
306 summer, and reaches its minimum in the middle of winter, at  $t = 273$  days.

307 Disturbance is modeled by a yearly recurrent cessation of feeding for a certain number of  
308 days per year. Consequently, disturbance is characterized by a disturbance period (number of  
309 days) and a starting date. Concerning the latter, we distinguish between summer (starting when  
310  $(t \bmod 365) = 91$  days) and winter disturbance (starting when  $(t \bmod 365) = 273$ ). During the  
311 disturbance period the resource ingestion rates of the calf and the female are set to zero.

312 Lactation is still possible during disturbance.

313

314 *Model analysis*

315 Model equations are implemented in the Escalator Boxcar Train (EBT; De Roos 1988) software  
316 package (available at <https://staff.fnwi.uva.nl/a.m.deroos/EBT/Software/index.html>). This  
317 package solves a set of ordinary differential equations describing the survival, growth and  
318 reproduction of the female and her calves. The integration of these ODEs is interrupted by events  
319 related to the onset of reproduction (when the pregnancy threshold is crossed), initiating of  
320 pregnancy, birth, weaning and death. Model output was processed and plotted using R software

321 with the `ggplot2` package (Wickham 2016, R Core Team 2017). The EBT model implementation  
322 file and R code to create the figures are available at (*bitbucket repository link here*).

323 We start off by illustrating the consequences of an increase in disturbance period on the life  
324 history of the female pilot whale and her calves by using the fixed life expectancy of 60 years. In  
325 the same setting, we explore the consequences of seasonal variation in resource density and  
326 differences in the timing of disturbance (summer vs. winter). With the fixed life expectancy, the  
327 number of weaned calves during the female's lifetime provides an upper estimate of the  
328 reproductive capacity. To arrive at a representative estimate of  $R_0$  we use the randomly  
329 determined life expectancy and average the lifetime reproductive output of the female across  
330 1000 simulated life histories. In addition to  $R_0$ , we calculate the following life history statistics:  
331 mean age at death as a measure of life expectancy, mean percentage of calves that survive until  
332 weaning age, mean female age at first reproduction, mean female age at which first calf is  
333 weaned (age at first weaning) and the mean time between different birth events (inter-birth  
334 interval). Basic nonparametric bootstrapping with 1000 resamples was used to calculate the  
335 mean and 95% confidence intervals of these life history statistics. This procedure is repeated for  
336 nine different values for mean annual resource density ( $\bar{R} = 1.6, 1.7, 1.8, 2.0, 2.2, 2.4, 2.6, 2.8,$   
337  $3.0$ ), four levels of resource seasonality ( $A = 0, 0.15, 0.3, 0.45$ ), 11 disturbance periods ( $0, 5, 10,$   
338  $15, 20, 25, 30, 35, 40, 45, 50$ ), and two different disturbance seasons ('summer' vs. 'winter').  
339

340 **Results**

341 *Undisturbed pilot whale life history*

342 Female reserve mass increases with age, although high lactation costs temporarily decrease  
343 reserve mass (Figure 2, for mean annual resource density  $\bar{R} = 1.8$ ). Outside lactation periods,

344 female reserve mass approaches an equilibrium value that is slightly below the target reserve  
345 threshold, which is a constant fraction of total mass ( $\rho W$ ). Structural mass is the main  
346 component of total mass and increases with age according to the Von Bertalanffy function (Table  
347 1). This drives the increasing asymptotic trend of reserve mass with age. Furthermore, reserve  
348 mass itself also contributes to total mass and the target and starvation reserve thresholds  
349 therefore also depend on reserve mass. Effectively, an increase in reserve mass triggers an  
350 increase in the target reserve threshold, although this increase is disproportionately smaller due to  
351 the large contribution of structural mass to total mass. When pregnant, the target and starvation  
352 reserve thresholds of the female are increased due to the contribution of fetal mass to total mass.  
353 The increase in target reserve threshold will lead to a higher feeding effort and in this way cover  
354 gestation costs. Figure 2a shows that reserve mass stays approximately constant during  
355 pregnancy, although the target reserve mass peaks due to the contribution of fetal mass.

356 Without disturbance, the reserve threshold for initiation of pregnancy is crossed for the  
357 first time at an age of 6.5 years and first birth occurs at age 8.7 years (Figure 2a). During the first  
358 lactation period the depletion of the female's reserve mass is most pronounced, as the female's  
359 structural mass is still developing and the absolute amount of reserves she can carry is limited.  
360 Female age also affects the inter-birth interval. After the first lactation period the female is  
361 "resting" and initiation of pregnancy only occurs  $T_D = 445$  days after the day she enters the  
362 waiting period (crosses the pregnancy threshold). During subsequent lactation periods the  
363 female's reserve mass stays above the pregnancy threshold and she already enters the waiting  
364 period within the last year of lactation. Consequently, there are only  $T_D - 364 = 81$  days  
365 between the weaning of a calf and initiation of the next pregnancy. Assuming that the female  
366 survives until age 60, she is able to wean 11 calves (5.5 females on average, Figure 2a). This

367 maximum reproductive potential is controlled more by the duration of the different reproductive  
368 phases (waiting, gestation and lactation) than by resource density. Increasing resource density  
369 from 1.8 to 5.0 would only lead to one extra calf being successfully weaned, setting the  
370 maximum reproductive potential to 12 calves (6 females on average).

371 In contrast to the female, reserve masses of the calves closely approximate their target  
372 reserve threshold (Figure 2a). Consequently, calves have a higher relative reserve mass than  
373 females (max. values 0.305 vs. 0.277, respectively). Since the target reserve threshold ( $\rho = 0.3$ )  
374 is independent of individual age or reproductive status, the high body condition of calves is an  
375 emergent property of the model and stems from the fact that calves benefit from two food  
376 sources simultaneously (resource feeding and lactation).

377 Some aspects of the bio-energetics of an undisturbed, fully-grown female and her calf are  
378 listed in table 2. When fully-grown the female has a structural mass of 672 kg and her reserve  
379 mass varies between 217 and 257 kg., depending on whether she is pregnant, lactating or  
380 recovering from lactation. In the latter case, the female awaits new implantation, but her reserve  
381 mass is still increasing. In comparison, if the female did not engage in reproductive activity, her  
382 reserve mass would equilibrate over time at 260 kg, but this state is never reached. Field  
383 metabolic costs are  $103 \text{ MJ} \cdot \text{day}^{-1}$ . On average, lactation increases resource assimilation rate  
384 more than pregnancy (29% vs. 8.7%) and one year of lactation is around 4 times more expensive  
385 than one year of pregnancy (11,476 MJ vs. 2,880 MJ), accounting for a  $3 \text{ MJ} \cdot \text{day}^{-1}$  increase in  
386 metabolic rate during pregnancy. During the first year 91% of the calf's energy is derived from  
387 milk, and for the remainder of the lactation period milk provides 58% of its energy requirements  
388 (66% on average for the whole period).

389

390     *Effect of disturbance*  
391     The first effect of disturbance is reduced survival or death of calves born to young lactating  
392     females. Depending on the duration of disturbance, the first one or more calves of the female die  
393     before weaning. At a yearly recurrent disturbance period of 15 days (Figure 2b), the disturbance  
394     event within the first lactation period leads to starvation of both calf and female (reserve  
395     densities drop below their starvation thresholds in Figure 2b), resulting in death of the calf before  
396     weaning. During lactation of the second calf only the female experiences starvation at two  
397     recurrent disturbance events and the calf survives. As a consequence, the age of the female when  
398     she weans her first calf (age at first weaning) increases from 12 to 15.8 years with 15 days of  
399     disturbance. The increased mortality experienced by the female during the first two lactation  
400     periods only leads to a minor decrease in female life expectancy, compared to the scenario  
401     without disturbance (59.4 vs. 60.3 yrs.).

402         Besides causing pre-weaned death of calves of young females, 15 disturbance days per  
403     year also increases the inter-birth interval (Figure 2b). Except for the last four lactation periods,  
404     the female only crosses the pregnancy threshold when lactation is finished. During the last four  
405     lactation periods, she does cross the pregnancy threshold in the last year of lactation, but not  
406     immediately on the first day of this last year. The combined effect of the early death of the first  
407     calf and the prolonged time periods between birth and weaning events is that 15 days of recurrent  
408     disturbance reduces the reproductive potential of the female to 9 calves (4.5 females on average).

409         Increasing the disturbance period leads to the pre-weaned death of multiple calves and can  
410     substantially shorten female life expectancy. In Figure 2c, a yearly recurrent disturbance of 25  
411     days leads to pre-weaned death of the first 4 calves (age at first weaning increases to 24.8 years)  
412     and a reduction in life expectancy to 42 yrs. Starvation of the female mainly occurs during the

413 lactation periods of the calves that do survive, while the pre-weaned deaths of the first 4 calves  
414 only incur very short starvation periods. Age at first reproduction is only moderately affected by  
415 disturbance, and the average inter-birth interval actually decreases, because the early death of a  
416 calf allows the female to give birth to the next calf sooner.

417

418 *Resource seasonality and the effects of disturbance*

419 Similar to the effect of disturbance, resource seasonality also reduces the maximum reproductive  
420 potential of a female by causing pre-weaned death of calves of young females and reducing  
421 female life expectancy (Figure 3), although it also leads to a younger age at first reproduction.  
422 Low to moderate seasonality mainly leads to reduced calf survival and early death of the first one  
423 or more calves, while female survival is only slightly affected. At a high level of seasonality, the  
424 female is unable to wean any calf and dies at a young age herself (Figure 3g).

425 In addition to these direct effects, resource seasonality also aggravates the effect of  
426 disturbance and increases the importance of the timing of disturbance. As the seasonal variation  
427 in resource density becomes more pronounced, the consequences of summer and winter  
428 disturbance begin to diverge. At low to moderate seasonality, disturbance in winter leads to more  
429 pre-weaned deaths of calves compared to summer disturbance (Figure 3), with no calves being  
430 successfully weaned with winter disturbance and a resource amplitude of 0.3. Also, the female  
431 suffers from starvation more with winter disturbance and this leads to lower female life  
432 expectancy. At high resource seasonality (0.45), the difference between summer disturbance and  
433 no disturbance is almost undetectable, while winter disturbance leads to death of the female  
434 during the first pregnancy. These different responses arise because in environments with

435 seasonal resource fluctuations, winter disturbance happens when resource density is already low,  
436 while summer disturbance occurs in periods when resources are relatively abundant.

437 In all cases where the calf dies before the age at weaning, it does so in the first phase of  
438 lactation. If a calf survives this initial vulnerable period, it is able to withstand successive  
439 disturbance events and survives until the age at weaning. This is especially true for calves of  
440 older females that have more reserves. In addition, older calves also carry more reserves  
441 themselves and have the ability to feed on the resource independently when the mother ceases  
442 milk supply.

443

444 *Overview of disturbance effects*

445 With a resource seasonality of 0.3, the disturbance duration that leads to population decline  
446 ( $R_0 < 1$ ) is approximately 3.3 times higher when disturbance happens in summer, compared to  
447 when disturbance happens in winter (Figure 4, with  $\bar{R} = 2.0$ ). With winter disturbance, mean  
448 female lifetime reproductive output, mean proportion of weaned calves and mean female life  
449 expectancy decline if disturbance duration exceeds 5 days per year. For summer disturbance, a  
450 decline in these life history statistics only occurs beyond 20 days of disturbance per year. The  
451 mean and variance of age at first weaning increase with disturbance duration and this happens  
452 more rapidly for winter disturbance compared to summer disturbance. No calves are successfully  
453 weaned if disturbance exceeds 20 days in winter, or 40 days in summer. The increasing number  
454 of pre-weaned calf deaths lead to a decrease in the mean inter-birth interval. The age at first  
455 reproduction is only marginally affected by disturbance. Variance in age at first reproduction is  
456 zero, since the randomly distributed life expectancy does not affect when the female's reserve  
457 mass crosses the pregnancy threshold.

458       The difference between summer and winter disturbance is most apparent at intermediate  
459   levels of resource seasonality. A lack of strong seasonal differences in resource density leads to  
460   similar responses between summer and winter disturbance, with a predicted population decrease  
461   beyond 25 days of disturbance per year (Appendix S2: Figure S1). Strong resource seasonality  
462   has itself a detrimental effect on lifetime reproductive output by diminishing the proportion of  
463   successfully weaned calves. In this case, disturbance will further reduce female life expectancy  
464   (Appendix S2: Figure S1).

465       The sequence of life history changes with increasing disturbance period is consistent  
466   between different levels of resource seasonality and disturbance in winter vs. summer. Using the  
467   output from the life history simulations with random life expectancy (Figure 4 and Appendix S2:  
468   Figure S1), we plot the life history statistics relative to the value of each statistic at zero  
469   disturbance period in Figure 5. This shows that changes in the age at first reproduction and the  
470   inter-birth interval are relatively minor. The main change that drives decreasing lifetime  
471   reproductive output seems to be the pre-weaned death of the first few calves, as reflected by the  
472   decrease in the proportion of successfully weaned calves and the increase in age at first weaning.  
473   Onset of changes in female life expectancy occur at a slightly higher disturbance duration.  
474   However, independent of disturbance season and resource seasonality, the changes in the  
475   female's reproductive success with increasing disturbance occur at broadly the same disturbance  
476   durations as changes in female survival (Figure 5).

477

478   *Varying resource density*

479   The differential response to the timing of disturbance relates to the availability of resources to  
480   compensate for disturbance. Resource seasonality increases the resource availability in summer,

481 while it decreases resource availability in winter. Consequently, in seasonal environments the  
482 female and her calves can only compensate for disturbance when it happens in summer, when  
483 resources are relatively abundant. Since the effect of seasonality acts through temporal resource  
484 availability, mean resource density will affect this response. We explore the impact of mean  
485 resource density by calculating the amount of disturbance that is required to negatively impact  
486 lifetime reproductive output. This disturbance threshold value is quantified by estimating the  
487 disturbance period at which the lifetime reproductive output is equal to 1 from a cubic smoothing  
488 spline applied to lifetime reproductive output data as a function of disturbance period. Figure 6  
489 shows how this threshold disturbance value depends on resource density, resource seasonality  
490 and the timing of disturbance (summer vs. winter). Overall, mean annual resource density  
491 increases the threshold disturbance value in a decelerating manner. Consequently, there exists a  
492 limit to which resource density can compensate for disturbance effects. Irrespective of overall  
493 resource density, higher levels of resource seasonality require shorter disturbance periods to  
494 negatively impact lifetime reproductive output, but only when disturbance happens in winter.  
495 When disturbance happens in summer, the effect of resource seasonality varies with resource  
496 density. At low mean resource density ( $< 2.5$ ), resource seasonality does not change the  
497 threshold disturbance value in any consistent way. However, at high resource density ( $> 2.5$ ), an  
498 increase in resource seasonality enables the female to withstand longer periods of disturbance  
499 before her lifetime reproductive output falls below 1. Consequently, at high mean annual  
500 resource density, resource seasonality aggravates the effect of disturbance in winter, while it  
501 attenuates the effect of disturbance in summer.

502

503 **Discussion**

504 The model shows that the impact of disturbance crucially depends on resource availability. First,  
505 high resource availability compensates for the effect of disturbance, but there is an upper limit to  
506 which this is possible. Second, the role of resource availability has important implications with  
507 respect to the timing of disturbance, as in many systems resource availability varies seasonally  
508 throughout the year, especially in temperate regions. Based on our results, the population can  
509 withstand a much longer period of disturbance in periods of abundant food (which we refer to as  
510 ‘summer’) compared to periods of low food (called ‘winter’ in our study). In the most seasonal  
511 environment considered here (a relative resource amplitude of 0.45), the disturbance duration  
512 that leads to population decline is on average 3.2 times longer for summer disturbance than for  
513 winter disturbance (Figure 6). This ratio between summer and winter disturbance decreases with  
514 mean annual resource density, as it equals 5.9 for the lowest resource density and 1.8 for the  
515 highest resource density.

516 A marked seasonal variation in body fat condition has been observed in Northeast Atlantic  
517 pilot whales, with whales being ‘fat’ in winter and ‘lean’ in summer (Lockyer 1993). According  
518 to Lockyer (1993), this seasonality in body fat condition is probably linked to resource  
519 availability, as it is independent of age and reproductive status. In general, the phenology of  
520 reproductive events such as mating, parturition and the subsequent onset of lactation might  
521 further increase seasonal variation in body condition (Lockyer 2007). During the mating season,  
522 males and females expend additional amounts of energy but may not be able to feed. Our model  
523 does not link reproductive events to certain periods within the year and we call the season of  
524 high resource availability ‘summer’, which leads to a peak in body condition during the end of  
525 summer and in autumn. The latter choice is of course arbitrary, the important point being that  
526 seasonal variation in body condition, either driven by resource availability or phenology of

527 reproductive events, should be taken into consideration when assessing the potential implications  
528 of disturbance on wildlife populations.

529 The most extreme form of seasonal variation in body condition are found in long-distance  
530 migratory species, such as baleen whales that do not feed during migration and rely on stored  
531 energy to provision migration, lactation and gestation (Alerstam et al. 2003, Stephens et al.  
532 2014). Due to this extreme lifestyle, disturbance affects such species differently compared to a  
533 medium-size cetacean like a pilot whale. For species that rely on stored energy reserves for  
534 reproduction and migration, disturbance that leads to cessation of feeding (as studied here) would  
535 impact animals only when it happens in the feeding grounds, which is where the energy reserves  
536 for the remainder of the migratory cycle are accumulated (Villegas-Amtmann et al. 2015).

537 Disturbance during migration mainly has consequences when it leads to increased metabolic  
538 costs, or separation between mother and calf. Pilot whales feed during the whole year and their  
539 fat reserves respond rapidly to environmental conditions. This makes them vulnerable to  
540 disturbance that leads to cessation of feeding during periods of low resource availability, and  
541 relatively invulnerable to disturbance when resources are high. Based on reserve dynamics in eq  
542 (1), one might expect that disturbance that increases metabolic costs will have a similar effect as  
543 cessation of feeding, as both processes lead to a decrease in available energy for lactation,  
544 gestation and growth (Figure 1). However, one difference between the two forms of disturbance  
545 is that compensatory feeding can occur simultaneously with disturbance that increases metabolic  
546 costs, but it can only occur after the event if disturbance disrupts feeding.

547

548 *The progression of disturbance effects*

549 Independent of resource density or seasonality, an increasing disturbance duration leads to a  
550 sequence of changes in the female's life history. As shown in Figure 5, the changes in age at first  
551 reproduction and inter-birth interval are relatively minor compared to the increase in age at first  
552 weaning and the decrease in percentage of successfully weaned calves. This indicates that the  
553 initial effect of disturbance is to reduce survival of calves produced early in the life of the  
554 female. Longer periods of disturbance then lead to a decrease in female life expectancy. While  
555 the decrease in reproductive ability, as measured by the proportion of successfully weaned  
556 calves, might precede the onset of negative effects of disturbance on survival, the changes in  
557 both life history processes occur over a broadly similar range of disturbance durations. As can be  
558 seen from Figures 2 and 3, the negative effects of disturbance on female survival in all cases  
559 involves the female crossing the starvation threshold when lactating. Although milk supply  
560 ceases at this point, continuing disturbance will inevitably increase starvation mortality and  
561 hence decrease life expectancy. Consequently, disturbance has concurrent effects on female  
562 reproduction and survival, because survival is only affected if the female is reproductively active  
563 (lactating).

564 According to our results, young lactating females and their calves are the most sensitive  
565 subgroup in the population. When young, the female is still growing and the size of her reserves  
566 is limited by her structural capacity. During first lactation, the female in a non-seasonal  
567 environment loses maximally 57 kg of reserves, which equals 35% of the reserve mass at the  
568 start of lactation and 9% of total mass (Figure 2a). In the same environment, a fully-grown  
569 female loses maximally 45 kg of reserves during lactation (Table 2), equaling 18% of initial  
570 reserve mass and 4.6% of total mass. It must be noted, however, that the impact of lactation on  
571 reserve mass varies with resource availability. Under high resource availability, reserve mass

572 changes only little with reproductive status. Data from pilot whales catches indicate that pregnant  
573 females are heavier than lactating ones, but this relationship was not significant (Lockyer 1993).  
574 In North Atlantic right whales, blubber layer was thinner during lactation and then thickened  
575 with time after weaning (Miller et al. 2011). Rolland *et al.* (2016) further discuss trends in body  
576 condition of North Atlantic right whales and make a similar classification of female reproductive  
577 status as used here, by distinguishing pregnant, lactating, resting and ‘available’ females  
578 (corresponding to our ‘waiting’ category). Similar to our model simulations (Figure 2 and 3),  
579 body condition was higher in ‘available’ and ‘pregnant’ females, compared to ‘resting’ and  
580 ‘lactating’ females (Rolland et al. 2016). This has important implications for monitoring  
581 programs that focus on (female) body condition. Poor body condition might actually indicate that  
582 females are actively reproducing (lactating or recovering from lactation) and therefore  
583 contributing to population growth, rather than indicating that the population suffers from  
584 disturbance.

585 Because responses in the inter-birth interval and age at first reproduction are relatively  
586 small, changes in these life history statistics are likely to remain undetectable in most wildlife  
587 populations. Responses in these variables will be more pronounced when reproductive events are  
588 restricted to certain periods within the year. This often is the case in species that migrate from  
589 feeding to breeding grounds. However, pilot whales are reported to have seasonal reproductive  
590 activities (Lockyer 2007). In such cases, disturbance can lead to skipped breeding years if it  
591 interrupts mating or if reserve mass is insufficient at the onset of the breeding season. Although  
592 reproductive events can occur at any time of year in our model, seasonal resource fluctuations  
593 can also induce skipped breeding years and delay the age at first reproduction by one whole year.  
594 This mainly occurs for mean annual resource densities lower than the one used in Figure 4.

595 Incorporating the phenology of reproductive events in the model is expected to increase the  
596 occurrence of delayed reproduction and prolong the inter-birth interval with increasing  
597 disturbance duration for higher resource densities.

598

599 *Energetics*

600 Lockyer (1993) discusses the energetics of female pilot whales, based on morphometric and  
601 biochemical data, which allows a comparison with the outputs from our bioenergetics model  
602 (Table 2). Based on the multi-species equation of Innes *et al.* (1987), ingestion rate of cetaceans  
603 (in  $\text{kg} \cdot \text{day}^{-1}$ ) follows the power function of total body mass  $0.123M^{0.8}$ . Applying this formula  
604 to the range in total mass of the fully-grown female (Table 2) this leads to an ingestion rate of 28  
605 – 29  $\text{kg} \cdot \text{day}^{-1}$ . One of the main prey of pilot whales (the squid *Todarodes sagittatus*) has an  
606 energetic content of  $4.27 \text{ MJ} \cdot \text{kg}^{-1}$  and an assimilation efficiency around 90 to 95% (Desportes  
607 and Mouritsen 1993, Lockyer 1993, 2007). This brings the estimated energy assimilation rate to  
608  $108 - 118 \text{ MJ} \cdot \text{day}^{-1}$ , which compares well with our values for pregnant and recovering females  
609 (Table 2). Lockyer (1993) notes that sperm whales increase food intake by 5–10% when  
610 pregnant and by 32–62% when lactating, with higher values in growing females. Our model for  
611 pilot whales predicts an average 9% and 29% increase during pregnancy and lactating,  
612 respectively, which are reasonable considering that pilot whales have a longer lactation period  
613 than sperm whales (3.35 vs 2 years, respectively). Finally, Lockyer (1993) calculates the milk  
614 intake during the first year of lactation to be 9,539 MJ, and a corresponding cost of lactation for  
615 the female of 11,171 MJ. Although some of the data that lead to these estimates have been used  
616 to derive energetic parameters in our model, the similarity of these numbers with our modeled

617 outcomes (9,870 and 11,476 MJ, respectively, Table 2) suggests that the bioenergetics model  
618 captures key aspects of pilot whale energetics.

619

620 *The choice of disturbance scenarios*

621 The behavioral response to disturbance we have modeled in this paper (complete cessation of  
622 feeding for 24 hours) is more extreme than the observed responses of long-finned pilot whales  
623 exposed to military sonar under experimental conditions (Sivle et al. 2012, Miller 2012, Isojunno  
624 et al. 2017). However, more extreme responses to actual navy exercises involving sonar have  
625 been documented in other medium-sized cetaceans (e.g. beaked whales - McCarthy et al. 2011,  
626 Falcone et al. 2017), and we chose to model an extreme response in order to provide a clear  
627 picture of the potential effects of lost foraging opportunities on pilot whale life histories. For  
628 similar reasons, we modeled longer disturbance durations as continuous periods during which no  
629 foraging was possible. As a result, disturbed animals could not compensate for lost foraging  
630 opportunities until all disturbance had ended. In practice, individuals within a population are  
631 likely to be exposed to different, time-varying patterns of disturbance that will probably have a  
632 less profound effect on survival and reproduction than we observed in our simulations. The  
633 framework described here can be readily adapted to investigate the potential effects of these real-  
634 world disturbances, provided their nature can be accurately described.

635

636 *Conclusions*

637 We used a bio-energetics approach to model the life history of a pilot whale female and her  
638 calves. With this model, we study how increasing levels of disturbance affect female life history  
639 and calf survival and how the consequences of disturbance depend on resource availability and

640 its variation through time. Although the model was specifically parameterized and tailored for  
641 long-finned pilot whales, its structure is general enough to represent other (marine) mammals if  
642 appropriate data on life history and energetics are available. In fact, a similar bio-energetics  
643 model with the same general structure (Figure 1) was used to describe the dynamics of a  
644 population of ungulates living in a grassland environment with seasonally varying productivity  
645 (De Roos et al. 2009). The same model could therefore be used to provide insights into the  
646 general consequences of disturbance. If more detailed information is available, it can be used to  
647 provide management advice for specific species or populations.

648

## 649 **Acknowledgments**

650 This research was supported by the Office of Naval Research grant N00014-16-1-2858:  
651 "PCoD+: Developing widely-applicable models of the population consequences of disturbance".  
652 VH and AMdR benefitted from funding from the European Research Council under the  
653 European Union's Seventh Framework Programme (FP/2007-2013) / ERC Grant Agreement No.  
654 322814 awarded to AMdR.

655

## 656 **Literature Cited**

657 Alerstam, T., A. Hedenstrom, and S. Akesson. 2003. Long-distance migration: evolution and  
658 determinants. *Oikos* 103:247–260.

659 Baird, R. W., J. F. Borsani, M. B. Hanson, and P. L. Tyack. 2002. Diving and night-time  
660 behavior of long-finned pilot whales in the Ligurian Sea. *Marine Ecology Progress Series*  
661 237:301–305.

- 662 Barlow, J., and P. Boveng. 1991. Modeling Age-Specific Mortality for Marine Mammal  
663 Populations. *Marine Mammal Science* 7:50–65.
- 664 Bloch, D., C. Lockyer, and M. Zachariassen. 1993. Age and Growth Parameters of the Long-  
665 Finned Pilot Whale off the Faroe Islands. Report of the International Whaling  
666 Commission, Special Issue 14:163–207.
- 667 Braithwaite, J. E., J. J. Meeuwig, and M. R. Hipsey. 2015. Optimal migration energetics of  
668 humpback whales and the implications of disturbance. *Conservation Physiology* 3:cov001–  
669 15.
- 670 Caswell, H. 2001. *Matrix Population Models*. Second edition. Sunderland: Sinauer.
- 671 Christiansen, F., and D. Lusseau. 2015. Linking Behavior to Vital Rates to Measure the Effects  
672 of Non-Lethal Disturbance on Wildlife. *Conservation Letters* 8:424–431.
- 673 Costa, D. P., L. Schwarz, P. Robinson, R. S. Schick, P. A. Morris, R. Condit, D. E. Crocker, and  
674 A. M. Kilpatrick. 2016. A Bioenergetics Approach to Understanding the Population  
675 Consequences of Disturbance: Elephant Seals as a Model System. Pages 161–169 in A. N.  
676 Popper and A. Hawkins, editors. *The Effects of Noise on Aquatic Life II*. Springer New  
677 York, New York, NY.
- 678 Cox, T. M., T. J. Ragen, A. J. Read, E. Vos, R. W. Baird, K. Balcomb, J. Barlow, J. Caldwell, T.  
679 Cranford, L. Crum, A. D'Amico, G. D'Spain, A. Fernandez, J. Finneran, R. Gentry, W.  
680 Gerth, F. Gulland, J. Hildebrand, D. Houser, T. Hullar, P. D. Jepson, D. Ketten, C. D.  
681 MacLead, P. Miller, S. Moore, D. C. Mountain, D. Palka, P. Ponganis, S. Rommel, T.  
682 Rowles, B. Taylor, P. Tyack, D. Wartzok, R. Gisinier, J. Mead, and L. Benner. 2006.  
683 Understanding the impacts of anthropogenic sound on beaked whales. *Journal of Cetacean  
684 Research and Management* 7:177–187.

- 685 De Roos, A. M. 1988. Numerical methods for structured population models: The Escalator  
686 Boxcar Train. *Numerical Methods for Partial Differential Equations* 4:173–195.
- 687 De Roos, A. M., N. Galic, and H. Heesterbeek. 2009. How resource competition shapes  
688 individual life history for nonplastic growth: ungulates in seasonal food environments.  
689 *Ecology* 90:945–960.
- 690 DeRuiter, S. L., B. L. Southall, J. Calambokidis, W. M. X. Zimmer, D. Sadykova, E. A. Falcone,  
691 A. S. Friedlaender, J. E. Joseph, D. Moretti, G. S. Schorr, L. Thomas, and P. L. Tyack.  
692 2013. First direct measurements of behavioural responses by Cuvier's beaked whales to  
693 mid-frequency active sonar. *Biology Letters* 9:20130223–20130223.
- 694 Desportes, G., and R. Mouritsen. 1993. Preliminary Results on the Diet of Long-Finned Pilot  
695 Whales off the Faroe Islands. Report of the International Whaling Commission, Special  
696 Issue 14:305–324.
- 697 Dolman, S. J., E. Pinn, R. J. Reid, J. P. Barley, R. Deaville, P. D. Jepson, M. OConnell, S.  
698 Berrow, R. S. Penrose, P. T. Stevick, S. Calderan, K. P. Robinson, R. L. Brownell, and M.  
699 P. Simmonds. 2010. A note on the unprecedented strandings of 56 deep-diving whales  
700 along the UK and Irish coast. *Marine Biodiversity Records*:1–11.
- 701 Falcone, E. A., G. S. Schorr, S. L. Watwood, S. L. DeRuiter, A. N. Zerbini, R. D. Andrews, R. P.  
702 Morrissey, and D. J. Moretti. 2017. Diving behaviour of Cuvier's beaked whales exposed  
703 to two types of military sonar. *Royal Society Open Science* 4:170629–21.
- 704 Fleishman, E., D. P. Costa, J. Harwood, S. Kraus, D. Moretti, L. F. New, R. S. Schick, L. K.  
705 Schwarz, S. E. Simmons, L. Thomas, and R. S. Wells. 2016. Monitoring population-level  
706 responses of marine mammals to human activities. *Marine Mammal Science* 32:1004–  
707 1021.

- 708 Friedlaender, A. S., E. L. Hazen, J. A. Goldbogen, A. K. Stimpert, J. Calambokidis, and B. L.  
709 Southall. 2016. Prey-mediated behavioral responses of feeding blue whales in controlled  
710 sound exposure experiments. *Ecological Applications* 26:1075–1085.
- 711 Halpern, B. S., S. Walbridge, K. A. Selkoe, C. V. Kappel, F. Micheli, C. D'Agrosa, J. F. Bruno,  
712 K. S. Casey, C. Ebert, H. E. Fox, R. Fujita, D. Heinemann, H. S. Lenihan, E. M. P. Madin,  
713 M. T. Perry, E. R. Selig, M. Spalding, R. Steneck, and R. Watson. 2008. A Global Map of  
714 Human Impact on Marine Ecosystems. *Science* 319:948–952.
- 715 Harwood, J., and K. Stokes. 2003. Coping with uncertainty in ecological advice: lessons from  
716 fisheries. *Trends in Ecology & Evolution* 18:617–622.
- 717 Harwood, J., S. King, C. Booth, C. Donovan, R. S. Schick, L. Thomas, and L. New. 2016.  
718 Understanding the Population Consequences of Acoustic Disturbance for Marine  
719 Mammals. Pages 417–423 in A. N. Popper and A. Hawkins, editors. *The Effects of Noise*  
720 on Aquatic Life II. Springer New York, New York, NY.
- 721 Heide-Jorgensen, M. P., D. Bloch, E. Stefansson, B. Mikkelsen, L. H. Ofstad, and R. Dietz.  
722 2002. Diving behaviour of long-finned pilot whales *Globicephala melas* around the Faroe  
723 Islands. *Wildlife Biology* 8:307–313.
- 724 Innes, S., D. M. Lavigne, W. M. Earle, and K. M. Kovacs. 1987. Feeding Rates of Seals and  
725 Whales. *Journal of Animal Ecology* 56:115–130.
- 726 Isojunno, S., D. Sadykova, S. DeRuiter, C. Curé, F. Visser, L. Thomas, P. J. O. Miller, and C. M.  
727 Harris. 2017. Individual, ecological, and anthropogenic influences on activity budgets of  
728 long-finned pilot whales. *Ecosphere* 8:e02044–26.
- 729 Kleiber, M. 1975. *The fire of life: an introduction to animal energetics*. R.E. Krieger Pub. Co.,  
730 Huntington, N.Y.

- 731 Kooijman, S. A. L. M. 2010. Dynamic Energy Budget theory for metabolic organisation. Third  
732 edition. Cambridge University Press, Cambridge, UK.
- 733 Lika, K., and S. A. L. M. Kooijman. 2011. The comparative topology of energy allocation in  
734 budget models. *Journal of Sea Research* 66:381–391.
- 735 Lockyer, C. 1993. Seasonal Changes in Body Fat Condition of Northeast Atlantic Pilot Whales,  
736 and their Biological Significance. Report of the International Whaling Commission,  
737 Special Issue 14:325–350.
- 738 Lockyer, C. 2007. All creatures great and smaller: a study in cetacean life history energetics.  
739 *Journal of the Marine Biological Association of the UK* 87:1035–12.
- 740 Martin, A. R., and P. Rothery. 1993. Reproductive Parameters of Female Long-Finned Pilot  
741 Whales (*Globicephala melas*) Around the Faroe Islands. Report of the International  
742 Whaling Commission, Special Issue 14:263–304.
- 743 Maxwell, S. M., E. L. Hazen, S. J. Bograd, B. S. Halpern, G. A. Breed, B. Nickel, N. M.  
744 Teutschel, L. B. Crowder, S. Benson, P. H. Dutton, H. Bailey, M. A. Kappes, C. E. Kuhn,  
745 M. J. Weise, B. Mate, S. A. Shaffer, J. L. Hassrick, R. W. Henry, L. Irvine, B. I.  
746 McDonald, P. W. Robinson, B. A. Block, and D. P. Costa. 2013. Cumulative human  
747 impacts on marine predators. *Nature Communications* 4:2688.
- 748 McCarthy, E., D. Moretti, L. Thomas, N. DiMarzio, R. Morrissey, S. Jarvis, J. Ward, A. Izzi, and  
749 A. Dilley. 2011. Changes in spatial and temporal distribution and vocal behavior of  
750 Blainville's beaked whales (*Mesoplodon densirostris*) during multiship exercises with mid-  
751 frequency sonar. *Marine Mammal Science* 27:E206–E226.

- 752 McHuron, E. A., D. P. Costa, L. Schwarz, and M. Mangel. 2016. State-dependent behavioural  
753 theory for assessing the fitness consequences of anthropogenic disturbance on capital and  
754 income breeders. *Methods in Ecology and Evolution* 8:552–560.
- 755 McHuron, E. A., L. K. Schwarz, D. P. Costa, and M. Mangel. 2018. A state-dependent model for  
756 assessing the population consequences of disturbance on income-breeding mammals.  
757 *Ecological Modelling* 385:133–144.
- 758 Miller, C. A., D. Reeb, P. B. Best, A. R. Knowlton, M. W. Brown, and M. J. Moore. 2011.  
759 Blubber thickness in right whales *Eubalaena glacialis* and *Eubalaena australis* related  
760 with reproduction, life history status and prey abundance. *Marine Ecology Progress Series*  
761 438:267–283.
- 762 Miller, P. 2012. The Severity of Behavioral Changes Observed During Experimental Exposures  
763 of Killer (*Orcinus orca*), Long-Finned Pilot (*Globicephala melas*), and Sperm (*Physeter*  
764 *macrocephalus*) Whales to Naval Sonar. *Aquatic Mammals* 38:362–401.
- 765 National Research Council. 2003. Ocean Noise and Marine Mammals. The National Academies  
766 Press, Washington, DC.
- 767 National Research Council. 2005. Marine Mammal Populations and Ocean Noise. Pages 1–143.  
768 National Academies Press, Washington, DC.
- 769 New, L. F., D. J. Moretti, S. K. Hooker, D. P. Costa, and S. E. Simmons. 2013. Using Energetic  
770 Models to Investigate the Survival and Reproduction of Beaked Whales (family *Ziphiidae*).  
771 *PLoS ONE* 8:e68725–14.
- 772 New, L. F., J. S. Clark, D. P. Costa, E. Fleishman, M. A. Hindell, T. Klanjšček, D. Lusseau, S.  
773 Kraus, C. R. McMahon, P. W. Robinson, R. S. Schick, L. K. Schwarz, S. E. Simmons, L.  
774 Thomas, P. Tyack, and J. Harwood. 2014. Using short-term measures of behaviour to

- 775 estimate long-term fitness of southern elephant seals. *Marine Ecology Progress Series*  
776 496:99–108.
- 777 Parsons, E. C. M. 2017. Impacts of Navy Sonar on Whales and Dolphins: Now beyond a  
778 Smoking Gun? *Frontiers in Marine Science* 4:78–11.
- 779 Parsons, E. C. M., S. J. Dolman, A. J. Wright, N. A. Rose, and W. C. G. Burns. 2008. Navy  
780 sonar and cetaceans: Just how much does the gun need to smoke before we act? *Marine  
781 Pollution Bulletin* 56:1248–1257.
- 782 Pirotta, E., C. G. Booth, D. P. Costa, E. Fleishman, S. D. Kraus, D. Lusseau, D. Moretti, L. F.  
783 New, R. S. Schick, L. K. Schwarz, S. E. Simmons, L. Thomas, P. L. Tyack, M. J. Weise,  
784 R. S. Wells, and J. Harwood. 2018a. Understanding the population consequences of  
785 disturbance. *Ecology and Evolution* 24:712–13.
- 786 Pirotta, E., M. Mangel, D. P. Costa, B. Mate, J. A. Goldbogen, D. M. Palacios, L. A. Hückstädt,  
787 E. A. McHuron, L. Schwarz, and L. New. 2018b. A Dynamic State Model of Migratory  
788 Behavior and Physiology to Assess the Consequences of Environmental Variation and  
789 Anthropogenic Disturbance on Marine Vertebrates. *The American Naturalist* 191:E40–  
790 E56.
- 791 R Core Team. 2017. R: A language and environment for statistical computing. R Foundation for  
792 Statistical Computing, Vienna, Austria. <https://www.R-project.org/>.
- 793 Rolland, R. M., R. S. Schick, H. M. Pettis, A. R. Knowlton, P. K. Hamilton, J. S. Clark, and S.  
794 D. Kraus. 2016. Health of North Atlantic right whales *Eubalaena glacialis* over three  
795 decades: from individual health to demographic and population health trends. *Marine  
796 Ecology Progress Series* 542:265–282.

- 797 Sivle, L. D., P. H. Kvadsheim, A. Fahlman, F.-P. Lam, P. Tyack, and P. Miller. 2012. Changes in  
798 dive behavior during naval sonar exposure in killer whales, long-finned pilot whales, and  
799 sperm whales. *Frontiers in Physiology* 3.
- 800 Stephens, P. A., A. I. Houston, K. C. Harding, I. L. Boyd, and J. M. McNamara. 2014. Capital  
801 and income breeding: the role of food supply. *Ecology* 95:882–896.
- 802 The International Whaling Commission. 1993. *Biology of Northern Hemisphere Pilot Whales*.  
803 Pages 1–493 (G. P. Donovan, C. H. Lockyer, and A. R. Martin, Eds.).
- 804 Tyack, P. L., W. M. X. Zimmer, D. Moretti, B. L. Southall, D. E. Claridge, J. W. Durban, C. W.  
805 Clark, A. D'Amico, N. DiMarzio, S. Jarvis, E. McCarthy, R. Morrissey, J. Ward, and I. L.  
806 Boyd. 2011. Beaked Whales Respond to Simulated and Actual Navy Sonar. *PLoS ONE*  
807 6:e17009–15.
- 808 Villegas-Amtmann, S., L. K. Schwarz, J. L. Sumich, and D. P. Costa. 2015. A bioenergetics  
809 model to evaluate demographic consequences of disturbance in marine mammals applied  
810 to gray whales. *Ecosphere* 6:art183–19.
- 811 Wang, J. Y., and S.-C. Yang. 2006. Unusual cetacean stranding event of Taiwan in 2004 and  
812 2005. *J. Cetacean Res. Manage.* 8:283–292.
- 813 Wensveen, P. J., A. M. von Benda-Beckmann, M. A. Ainslie, F.-P. A. Lam, P. H. Kvadsheim, P.  
814 L. Tyack, and P. J. O. Miller. 2015. How effectively do horizontal and vertical response  
815 strategies of long-finned pilot whales reduce sound exposure from naval sonar? *Marine*  
816 *Environmental Research* 106:68–81.
- 817 Wickham, H. 2016. *ggplot2: Elegant Graphics for Data Analysis*. Springer-Verlag, New York.
- 818

**Table 1:** Overview of most important model components. Variables are indicated with ‘~’.

Variable, parameter	Unit	Description	Value
$t$	days	Time	~
Resource			
$R$	$\text{MJ} \cdot \text{m}^{-3}$	Resource density	$R = \bar{R} \left( 1 + A \sin \left( \frac{2\pi t}{365} \right) \right)$
$\bar{R}$	$\text{MJ} \cdot \text{m}^{-3}$	Annual mean resource density	1.6 – 3.0
$A$	–	Relative amplitude of seasonal resource variation	0, 0.15, 0.3, 0.45
Age			
$a$	days	Individual age	~
$\tau_p$	days	Time since conception	~
$T_P$	days	Gestation period	365
$T_L$	days	Lactation period	1223
$T_D$	days	Waiting period	445
Reserves			
$F$	kg	Reserve density	~
	kg	Pregnancy threshold	$\rho_s W + F_{\text{neonate}}$
$F_{\text{neonate}}$	kg	Amount of reserves to create a newborn individual	61.45
	–	Body condition	$F/W$
$\rho$	–	Target body condition	0.3
$\rho_s$	–	Starvation threshold	0.15
Length			
$l(a)$	cm	Length-age relationship free-living individual	$l_\infty - (l_\infty - l_b)e^{-ka}$
$l_b$	cm	Length at birth	177
$l_\infty$	cm	Asymptotic length	450
$k$	$\text{day}^{-1}$	Von Bertalanffy growth rate	0.00045
$l_p(\tau_p)$	cm	Length-age relationship fetus	$l_b \frac{\tau_p}{T_P}$
Structural mass			

---

$S(l)$	kg	Structural mass-length relationship	$\omega_1 l(a)^{\omega_2}$
$\omega_1$	$\text{kg}\cdot\text{cm}^{-\omega_2}$	Mass-length scaling constant	$8.5\cdot 10^{-5}$
$\omega_2$	—	Mass-length scaling exponent	2.6
Body mass			
$W(S, F, \tau_p)$	kg	Total body mass	$\begin{cases} S + F + S(l_p(\tau_p)) & \text{pregnant} \\ S + F & \text{otherwise} \end{cases}$
$W_M(S, F, \tau_p)$	kg	Maintenance body mass	$\begin{cases} S + \theta_F F + S(l_p(\tau_p)) & \text{pregnant} \\ S + \theta_F F & \text{otherwise} \end{cases}$
$\theta_F$	—	Relative maintenance costs of reserves	0.2

---

**Table 2:** Some aspects of the energetics of the modeled pilot whale female, living in an undisturbed, constant environment with resource density  $R = 1.8$  and other parameters as default (Appendix S1: Table S2). The female is fully grown (growth costs are zero) with a structural mass of 672 kg.

Quantity	Mean <sup>a</sup>	% Increased	Total <sup>b</sup>
Reserve mass			
At equilibrium	260	0 (reference value)	
Recovering <sup>c</sup>	245 (233 – 254)	-5.7% (-10 – -2.3)	
During pregnancy	257 (253 – 258)	-1.2% (-2.7 – -0.8)	
During lactation	217 (213 – 248)	-16% (-18 – -4.6)	
Resource assimilation			
For metabolism	103	0 (reference value)	
Recovering <sup>c</sup>	118 (111 – 126)	15% (7.8 – 22)	
During pregnancy	112 (106 – 123)	8.7% (2.9 – 19)	
During lactation	133 (116 – 134)	29% (13 – 30)	
Pregnancy costs			
Structural growth fetus	4.9 (0 – 13)		1,787
Metabolic rate during pregnancy	106 (104 – 111)	2.9% (1.0 – 7.7)	
Lactation costs			
First year	31 (29 – 44)		11,476
Whole period	30 (0.2 – 44)		36,210
Calf milk assimilation			
First year	27 (25 – 38)		9,870
Whole period	25 (0.2 – 38)		31,140
Calf resource assimilation			
First year	2.7 (0 – 7.1)		1,017
Whole period	13 (0 – 42)		16,338

<sup>a</sup> Mean (min – max) values for reserve mass are in kg and other values are rates in MJ · day<sup>-1</sup>.

<sup>b</sup> Total rates (in MJ) are integrated over the relevant period.

<sup>c</sup> The recovering female is waiting to become pregnant again, but her reserve mass still increases from the previous lactation period.

## Figure legends

**Figure 1:** Schematic overview of the Dynamic Energy Budget model that controls pilot whale life history. Boxes indicate different sources (green) and destinations (red) of energy flows (connecting lines). Incoming and outgoing energy flows are denoted by  $I_i$  and  $C_i$ , respectively.  $I_T$  and  $C_T$  represent total incoming and outgoing energy flow, the difference of which constitutes the reserve dynamics (blue). Solid lines represent energy flows for all individuals, while dashed lines are energy flows that depend on individual state. Modified from (De Roos et al. 2009).

*Permission for reprinting will be requested through the Copyright Clearance Center's RightsLink service upon acceptance.*

**Figure 2:** Reserve mass of the female and her calves as a function of female age for different disturbance periods (0, 15 & 25 days per year). Female reserve mass is colored according to reproductive status (as indicated). A non-pregnant and non-lactating female is coined ‘waiting’ when her reserve mass is above the pregnancy threshold (not shown) and she awaits implantation, otherwise she is coined ‘resting’. Target and starvation reserve thresholds are plotted for both the female (upper lines) and calves (lower lines) and are equal to total body mass multiplied by  $\rho = 0.3$  and  $\rho_s = 0.15$ , respectively. LRO = lifetime reproductive output (female offspring only), AfR = female age at first reproduction (yrs), AfW = female age at which first calf is weaned, LE = life expectancy (yrs) and IBI = inter-birth interval (yrs). A fixed life expectancy at birth of 60 years was used, which can only decrease due to additional starvation mortality. Mean annual resource density  $\bar{R} = 1.8$  and all other parameters at default values (Appendix S1: Table S2).

**Figure 3:** Reserve mass of the female and her calves as a function of female age for different resource amplitudes (0.15, 0.3 & 0.45, in different rows) and with either no disturbance (left

columns), 15 days of summer disturbance (middle columns) or 15 days of winter disturbance (right columns). Lines, life history statistics, color-coding and other parameters as in Figure 2. Only the first 30 years of female life are plotted as the female is fully-grown by that age and patterns of reserve dynamics do no longer change. As in Figure 2, a fixed life expectancy of 60 years was used and death at younger age results from experiencing starvation mortality.

**Figure 4:** Life history statistics as a function of disturbance period for both summer and winter disturbance. Each data point represents the mean of 1,000 life history simulations, each with a randomly determined life expectancy for both the female and each calf. Colors indicate bootstrapped 95% confidence intervals of the mean. LRO: lifetime reproductive output, Prop. weaned: proportion of calves that survive until weaning age, LE: life expectancy, AfR: age at first reproduction, AfW: female age at which first calf is weaned and IBI: inter-birth interval. The randomly determined life expectancy does not impose variation in age at first reproduction and for some data points at high disturbance values the lack of color bands indicates the coincidence of minimum and maximum values. Mean annual resource density  $\bar{R} = 2.0$  and resource seasonality  $A = 0.3$ . All other parameters at default values (Appendix S1: Table S2).

**Figure 5:** Relative change in the life history statistics as a function of summer (left) and winter (right) disturbance for four levels of resource seasonality (different rows, as indicated in panel labels). These lines are derived by dividing each data point by the mean value at zero days of disturbance, allowing a comparison between the magnitude of change in these life history statistics. Other parameters as in Figure 4.

**Figure 6:** The threshold disturbance value is the disturbance period at which the mean lifetime reproductive output of the female falls below 1 and is plotted as function of mean annual resource density (horizontal axis), for different levels of resource seasonality and either summer

or winter disturbance. Higher resource densities allow for longer periods of disturbance. Higher resource seasonality only does so when disturbance happens in summer while in winter resource seasonality increases vulnerability to disturbance.

**Figure 1**

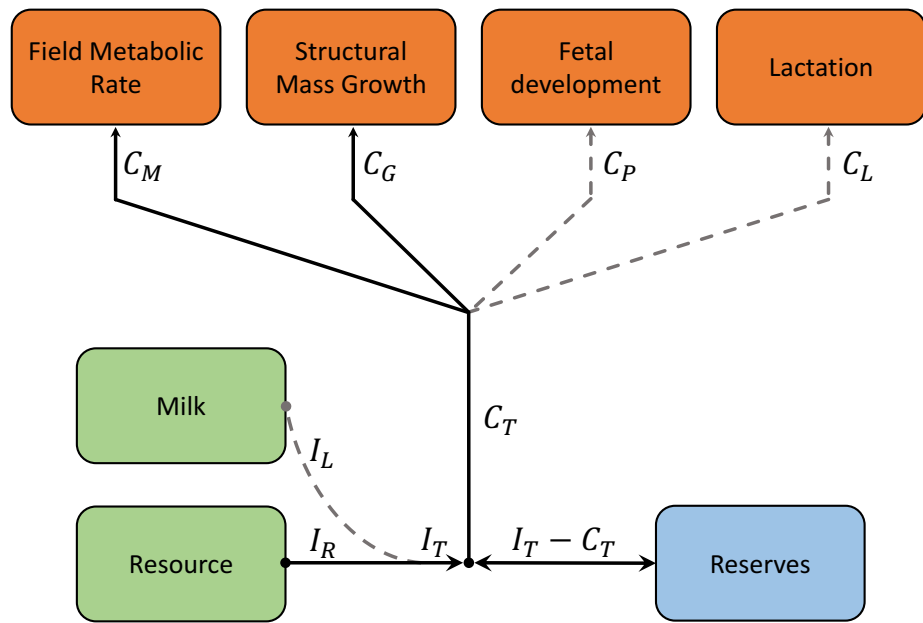


**Figure 2**

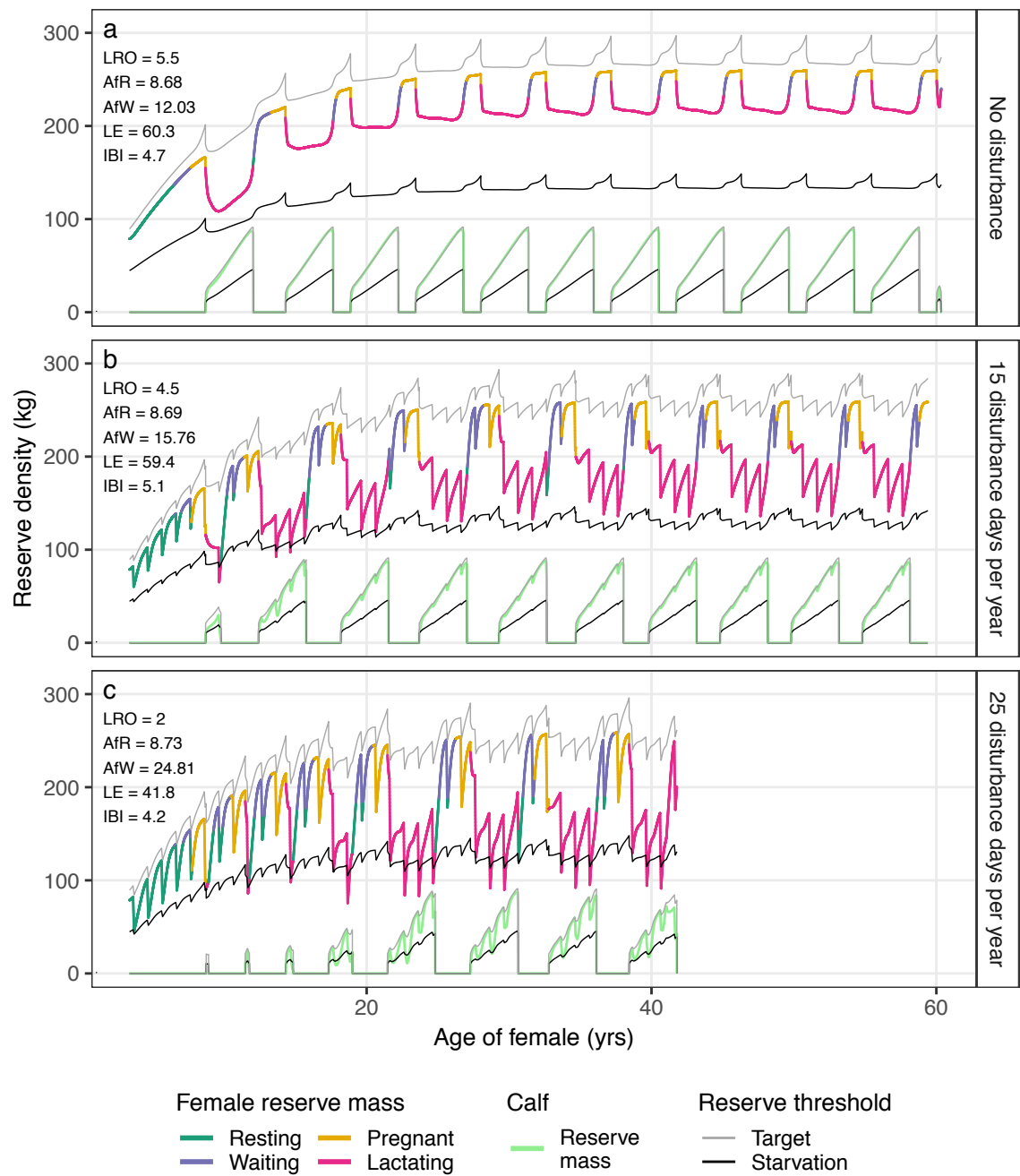


**Figure 3**

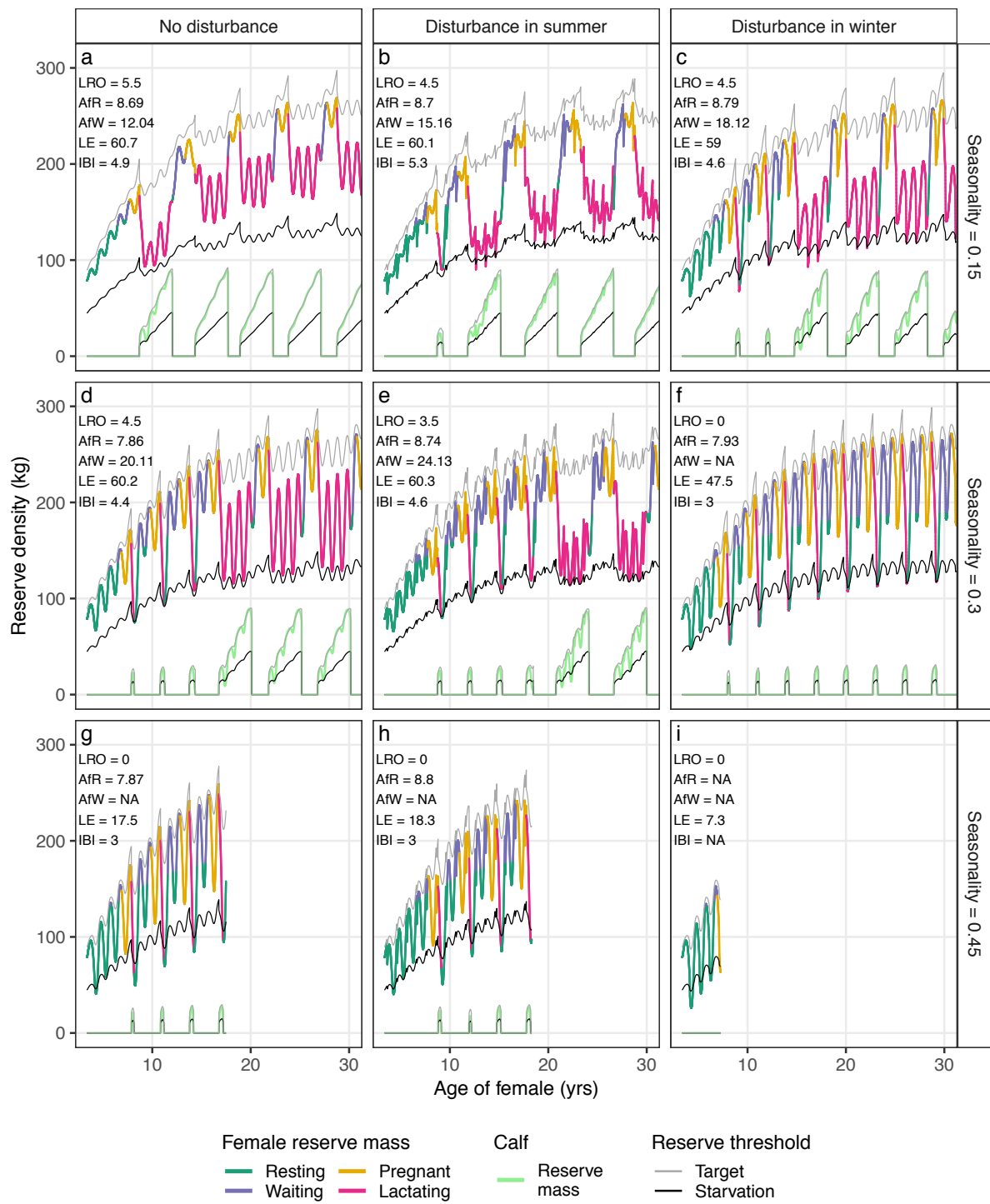


**Figure 4**

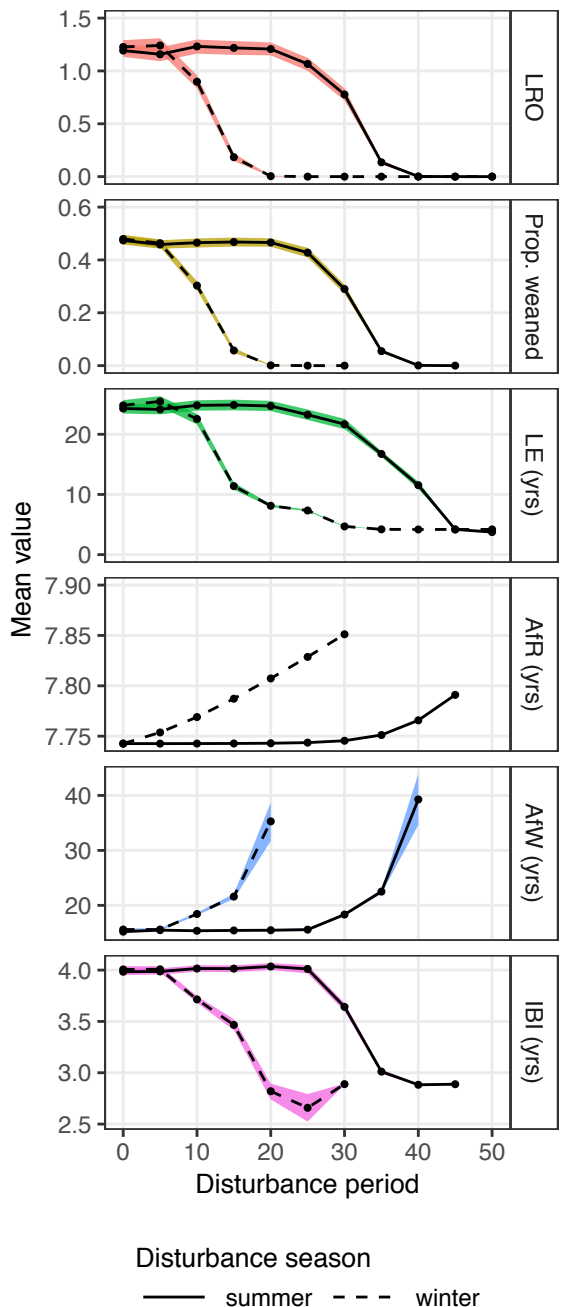


**Figure 5**

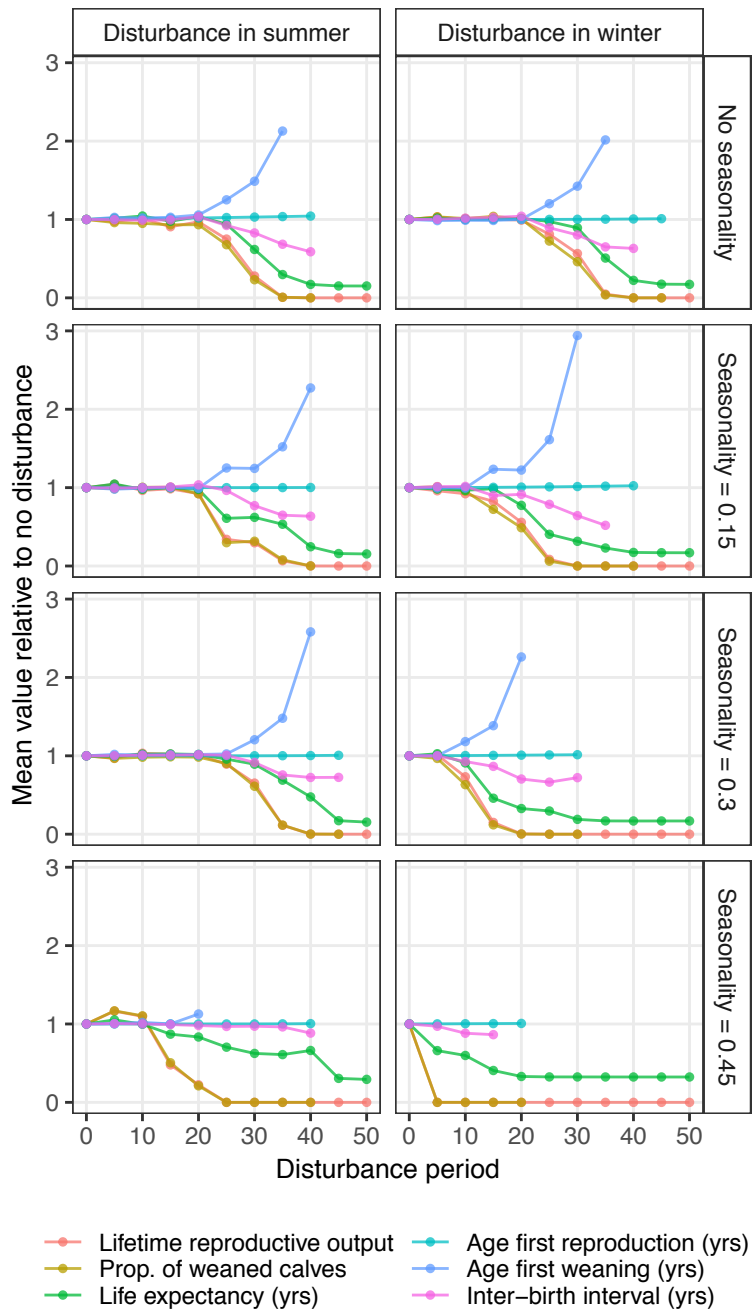
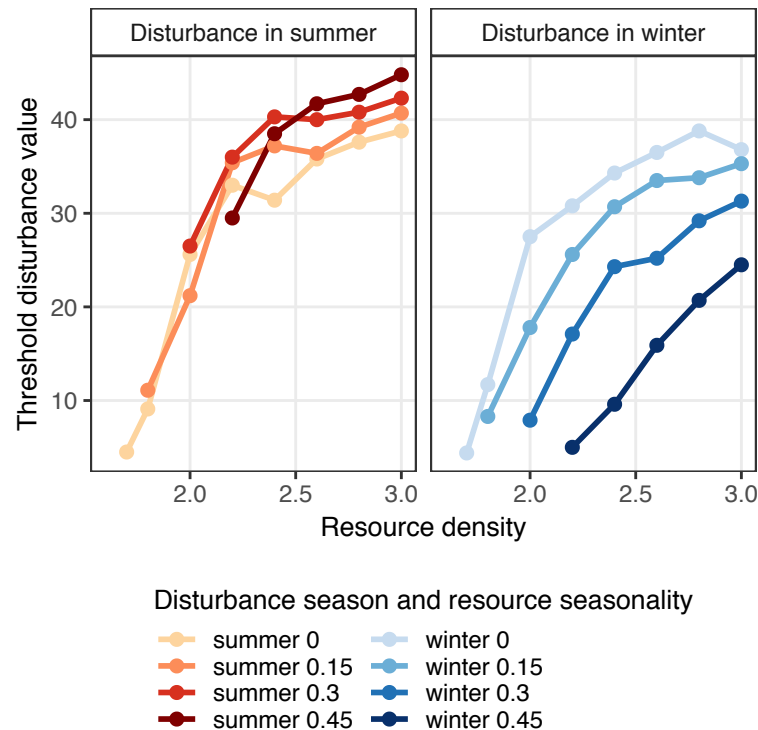


**Figure 6**



1   **Supporting Information.** Bio-energetic modeling of medium-sized  
2   cetaceans shows high sensitivity to disturbance in seasons of low resource supply  
3   *Vincent Hin, John Harwood & André M. de Roos.*

4   Ecological Applications

5

6   **Appendix S1**

7   *Model Description*

8   All model equations are summarized in Table S1, while the most important model features are  
9   listed in Table 1 of the main text. The two core individual-state (*i*-state) variables are age (*a* in  
10   days) and reserve mass (*F* in kg.). We also track the structural length (*l* in cm), structural mass  
11   (*S* in kg), total body mass (*W* in kg) and maintenance body mass (*W<sub>M</sub>* in kg) of each individual,  
12   but these quantities are all functions of age and/or reserve mass. For the female, we track  
13   whether she is waiting (0/1), pregnant (0/1) and lactating (0/1). When the female is pregnant, we  
14   track time since conception ( $\tau_p$ ). Eqs. 1-5 in Table S1 describe how the derived quantities  
15   depend on the core *i*-state variables of age and reserve mass.

16       Besides the specification of the *i*-states, the DEB model describes how the flow of energy  
17   depends on the *i*-state variables and their derived quantities. The different energy flows are  
18   represented by the lines connecting the different boxes in Figure 1 (main text) and their  
19   equations are shown in Table S1 (eqs 6-11). The resource assimilation rate is composed of four  
20   parts. The first describes a linear functional response ( $\phi_R R$ ). Here, quantities such as assimilation  
21   and conversion efficiencies as well as resource encounter rate and catch probability are captured  
22   in resource density *R* and the multiplication with scalar  $\phi_R$  only occurs to relate this resource

density to the rate of resource assimilation. Because  $R$  and  $\phi_R$  only enter the model through their product ( $\phi_R R$ ), the value of  $\phi_R$  on its own is arbitrary and will not affect model dynamics. The resource density  $R$  should be interpreted as the available amount of assimilated energy per unit of volume in the environment, while the product  $\phi_R R$  is the amount of assimilated energy acquired per day per unit of  $S^{2/3}$ . The second part of  $I_R$  describes the scaling of resource ingestion with structural whale mass to the two-thirds power,  $S^{2/3}$ . Taken together, the product  $\phi_R R S^{2/3}$  accounts for the maximum resource assimilation rate per individual whale, at resource density  $R$ . The third part is the first fraction in eq. (6) and discounts resource assimilation based on body condition  $\frac{F}{W}$ . This is a sigmoidal decreasing function of  $\frac{F}{W}$  and equals 0.5 at a body condition of  $\rho$  (see Figure S1b). The steepness is controlled by parameter  $\eta$ . The last component of  $I_R$  modifies the age-dependency of resource assimilation. This function increases from 0 at birth and asymptotically approaches 1 with increasing age (Figure S1c). The age at which this function equals 0.5 is controlled by parameter  $T_R$ , while the non-linearity is determined by  $\gamma$ .

Similar to the resource assimilation rate, the milk assimilation rate  $I_L$  also depends on a lactation scalar ( $\phi_L$ ), structural size ( $S^{2/3}$ ) and body condition ( $\frac{F}{W}$ ). However, the age-dependency of milk assimilation takes a different form. During the first year of lactation, calf age does not influence milk assimilation rate. Beyond the first year, the age-dependency term models an accelerating decline of milk assimilation with increasing age, up until the age at weaning, when the milk assimilation rate becomes zero (Figure S1d). The non-linearity of this component is controlled by parameter  $\xi_c$ . In addition, milk assimilation rate also depends on the milk provisioning by the female, which is a function of her body condition. Milk provisioning is represented by the last factor in eq. (7) (Table S1), where the  $i$ -state variables with subscript  $m$  belong to the female. This factor ensures that milk provisioning becomes zero if the body

46 condition of the female approaches the starvation threshold  $\rho_s$ , whereas milk provisioning equals  
47 1 if the female's body condition equals the target body condition  $\rho$  (Figure S1e). The non-  
48 linearity in this function is controlled by parameter  $\xi_m$ .

49 The different forms of energy expenditure are denoted by  $C_i$  and shown in eqs. (8-11) of  
50 Table S1. Field metabolic costs (eq. 8) are proportional to the  $3/4$ -power of maintenance body  
51 mass  $W_M$ , following (Kleiber 1975). As discussed in the main text, maintenance body mass  
52 discounts for the lower contribution of reserve mass to metabolic rate. The costs of growth (eq.  
53 9) follows from the derivative of structural mass with respect to age  $\left(\frac{ds(l(a))}{da}\right)$ , multiplied by the  
54 energetic costs of growing 1 kg of structural mass ( $\sigma_G$ ). Similarly, the costs of growing a fetus  
55 are proportional to the derivative of structural mass of the fetus with respect to time since  
56 conception  $\left(\frac{ds(l_p(\tau_p))}{d\tau_p}\right)$ , again with proportionality constant  $\sigma_G$  (Table S1: eq. 10). The function  
57  $C_p$  only covers the structural growth costs of the fetus, while the maintenance costs of the  
58 growing fetus are modeled by incorporating its mass into the maintenance body mass of the  
59 pregnant female. Finally, lactation costs are equal to the milk assimilation rate of the calf,  
60 corrected for the efficiency of lactation  $\sigma_L$  (Table S1; eq. 11). Here, the index  $c$  indicates that the  
61 variable belongs to the calf.

62 Three types of age-dependent mortality are captured by eq. (12) in Table S1. This equation  
63 was fitted to data of Bloch et al. (1993a) and provides an equal fit compared to an equation that  
64 describes the three forms of age-dependent mortality as three separate terms, but requiring an  
65 additional parameter. The age-dependent mortality function describes an age-independent  
66 background mortality rate for all individuals, a decreasing mortality rate for young individuals  
67 and an increasing mortality rate for older individuals (Figure S1f). Starvation mortality only

68 applies when body condition falls below the starvation threshold  $\rho_s$  and increases with  
69 decreasing body condition (eq. 13; Figure S1g). The scaling of this increase is determined by  
70 parameter  $\mu_s$ .

71 The life of the simulated female is initiated at her age at weaning ( $T_L = 1223$ ) and her  
72 survival therefore equals 1 at this point. Provided that the female's body condition remains above  
73  $\rho_s$ , survival is only decreased due to background mortality. The resulting age-dependent survival  
74 curve is plotted in Figure S1h. If her body condition drops below  $\rho_s$ , the female experiences a  
75 period of starvation mortality, which adds to the background mortality rate and thus decreases  
76 survival. Even if the female's body condition recovers above  $\rho_s$  she will have a lower age-  
77 dependent survival curve compared to the situation if starvation had not occurred (Figure S1h).  
78 Consequently, the life expectancy of a female that experiences starvation will be decreased.

79 The pregnancy threshold uses the amount of reserves that is required to produce a newly  
80 born calf  $F_{neonate}$ . This quantity is composed of two components (Table S1: eq. 14). The term  
81  $\frac{\sigma_G \omega_1 l_b^{\omega_2}}{\epsilon^-}$  accounts for the growth costs of the structural mass of the fetus, expressed in reserve  
82 mass of the female (hence the division by  $\epsilon^-$ ). The term  $\frac{\rho_s \omega_1 l_b^{\omega_2}}{(1-\rho_s)}$  accounts for the amount of  
83 reserves that the female transfers to the calf at birth. This quantity is such that the body condition  
84 of the newborn calf equals the starvation threshold.

85 The last equation in Table S1 describes how the seasonally varying resource density is  
86 modeled. For this we use a sine function such that resource density equals the yearly mean  
87 resource density at the start of each year ( $t = 0, 365$ , etc) and increases (Figure S1i). This  
88 corresponds to spring which is when we assume the female is initiated.

89

90 *Model Parameters*

91 Most model parameters are derived from the international research program on Northeast  
92 Atlantic long-finned pilot whales off the Faroe Islands, which was conducted between July 1986  
93 and July 1988 (Bloch et al. 1993b). The year-round drive-fisheries on the Faroe Islands resulted  
94 in detailed information on age and growth parameters (Bloch et al. 1993a), reproductive  
95 parameters (Martin and Rothery 1993) and bioenergetic parameters (Lockyer 1993) of a large  
96 number of pilot whales ( $n > 3000$ ). Some parameter values could not be derived directly from  
97 sources (e.g. lactation scalar  $\phi_L$ ) and these were based on reasonable biological assumptions and  
98 the values of other parameters. All model parameters with references to the sources used in their  
99 derivation are listed in Table S2.

100 Estimates of gestation and lactation periods are given by Martin and Rothery (1993) and  
101 amount to 12 months (365 days) and 40.2 months (1223 days), respectively. Lockyer (1993)  
102 suggests that during the first year of life, calves are solely dependent on milk, which gives  $T_N =$   
103 365. The duration of the waiting period was calculated by assuming that ovulation occurs once  
104 per year and has a chance of pregnancy of 82%. This latter chance is derived from the ratio  
105 between the inter-ovulation interval and the interval-birth interval (4.17 : 5.1, as reported by  
106 Martin and Rothery 1993). This leads to a waiting period of  $\frac{365}{0.82} = 445$  days. Estimates for the  
107 parameters describing the increase in resource feeding efficiency with age ( $T_R$  and  $\gamma$ ) are not  
108 available and we adopt  $T_R = 500$  and  $\gamma = 2$ . With these values, the resource feeding efficiency  
109 increases rapidly at first, equals  $\sim 86\%$  per cent at weaning age and asymptotically approaches  
110 100% (Figure S1c).

111 Bloch et al. (1993a their Table 7) report several estimates for length at birth and total mass  
112 at birth and we adopt their best estimates of  $l_b = 177$  cm and  $W_b = 75$  kg. Mean length-at-age  
113 data in Bloch et al. (1993a their Table 10) is used to fit parameters  $l_\infty$  and  $k$ . In the fitting

114 procedure, its assumed that the reported ages indicate the beginning of the age classes, which  
115 implies that the true mean ages are 0.5 years later. This age-transformation resulted in a  
116 satisfactory fit of a non-linear regression with parameters  $l_\infty = 450$  and  $k = 0.00045$ , while  
117 fixing  $l_b = 177$  (Figure S1a).

118 Energy densities for pilot whales at different ages as reported by Lockyer (1993) were used  
119 to estimate the length-structural mass relationship parameters  $\omega_1$  and  $\omega_2$ , and the target and  
120 starvation body condition parameters  $\rho$  and  $\rho_s$ . In this derivation, we use lipid proportion as an  
121 indication of the percentage of reserve mass of an individual. The fact that a part of the lipid  
122 content of an individual has a structural origin and cannot be mobilized without compromising  
123 survival is accounted for by setting the starvation threshold  $\rho_s > 0$ . Lipid proportion for calves is  
124 around 17% (Lockyer 1993), which makes structural mass at birth  $S_b = 75 \cdot (1 - 0.17) = 62$   
125 kg. Ultimate body mass is reported by Bloch et al. (1993a) as  $W_\infty = 1320$  kg for individuals  
126 with  $l_\infty = 512$  cm. According to Lockyer (1993), lipid content of these individuals is around  
127 25%, so by a similar calculation  $S_\infty = 990$  kg. This leads to a length-structural mass scaling  
128 exponent of  $\omega_1 = \ln\left(\frac{S_\infty}{S_b}\right)/\ln\left(\frac{l_\infty}{l_b}\right) = 2.6$ . Consequently, the length-structural mass scaling  
129 constant equals  $\omega_2 = 8.5 \cdot 10^{-5}$ . A large proportion of the lipid content of calves (17%)  
130 probably belongs to structural mass and cannot be used as energy reserve without endangering  
131 life. Based on this we adopt  $\rho_s = 0.15$ . This corresponds well to the observation that most pilot  
132 whales of the Faroese population have a body condition in the range 0.14 – 0.23 (Lockyer 1993).  
133 Since modeled reserve mass for females equilibrates below the target reserve threshold, we adopt  
134  $\rho = 0.30$  and  $\eta = 15$ .

135 Compared to the maintenance costs for structural mass, the maintenance costs of reserves  
136 are lower per unit body mass. This relative discounting is quantified with parameter  $\theta_F$ . DEB

137 theory argues that fat reserves do not require maintenance (Kooijman 2010), which implies that  
138  $\theta_F = 0$ . While the amount of basal metabolic costs of reserves might be limited, reserves can  
139 increase field metabolic costs by increasing energetic costs of locomotion and activity. This  
140 holds especially for marine mammals, in which large fat reserves can increase drag. We therefore  
141 adopt the conservative estimate of  $\theta_F = 0.2$ . Although maintenance costs of fetus mass might  
142 also be lower per unit mass than maintenance costs of structural mass, fetal maintenance also  
143 includes costs for the placenta as well as increased metabolic costs for the mother due to  
144 increased drag and activity costs. Consequently, no discounting for fetal metabolism was  
145 applied.

146 Field metabolic maintenance rate follows Kleiber's relationship (Kleiber 1975). The scalar  
147 of this relationship ( $\sigma_M$ ) was set to 0.75. This approximately represents a 2.5 multiple of basal  
148 metabolic rate, as proposed by Lockyer (1993). Costs of growth in structural mass (represented  
149 by  $\sigma_G$ ) includes both growth overheads and the energy assembled in the newly synthesized  
150 biomass. We derive an estimate for  $\sigma_G$  by combining Brody's (1968) equation for the heat of  
151 gestation ( $Q_G = 4400W(0)^{1.2}$  in kCal) with estimates of the energy densities of pilot whales as  
152 reported by Lockyer (1993). Heat of gestation for a 75 kg neonate amounts to 3274 MJ. This  
153 includes the fetal maintenance metabolic rate during the gestation period, which in our model  
154 amounts to  $\int_0^{T_p} \sigma_M \left( \omega_1 \left( l_b \frac{\tau_p}{T_G} \right)^{\omega_2} \right)^{0.75} d\tau_c = 1987$  MJ. Energy content of a 75 kg neonate is  
155 estimated to be  $7.95 \cdot 75 \cdot 1.25 = 745$  MJ. This estimate accounts for the placenta, which adds  
156 25% to the neonate mass and uses an energy density of fetus and placenta at birth of  $7.95 \text{ MJ} \cdot \text{kg}^{-1}$ .  
157 (Lockyer 1993). This implies a growth efficiency of  $745 / (3274 - 1987 + 745) = 0.366$ .  
158 Pilot whale calves have a considerably higher energy density of  $10.1 \text{ MJ} \cdot \text{kg}^{-1}$  (Lockyer 1993),

159 which results in  $\sigma_G = 27.4 \text{ MJ} \cdot \text{kg}^{-1}$ . Since the heat of gestation is likely to be an underestimate  
160 of the true costs of gestation we settle for a value of  $\sigma_G = 30 \text{ MJ} \cdot \text{kg}^{-1}$ .

161 The conversion efficiency parameter  $\sigma_L$  controls both the assimilation efficiency of milk by  
162 calves and the efficiency with which the mother produces milk from reserves. Lockyer (1993)  
163 notes that efficiency of milk assimilation is 95% and that mammary gland efficiency of milk  
164 production is 90%. Combining these estimates yields a value of  $\sigma_L = 0.86$ .

165 The lactation scalar  $\phi_L$  was parameterized such that the amount of energy expended in the  
166 first year of life (maintenance and growth costs) can be completely covered by milk suckling,  
167 which is reasonable for pilot whales (Lockyer 1993). Energy expended on maintenance during  
168 the first year follows from solving the integral:  $\int_0^{365} \sigma_M \left[ \left( 1 + \theta_F \frac{\rho}{1-\rho} \right) \omega_1 l(a)^{\omega_2} \right]^{0.75} da =$   
169 7808 MJ, in which it is assumed that  $F/W = \rho$  and that  $l(a)$  follows eq. 2 in Table S1. Based  
170 on eqs. 2 and 3, structural growth during the first year equals 41 kg and corresponding growth  
171 costs amount to 1230 MJ. If milk assimilation covers all these expenses then, assuming  $F/W =$   
172  $\rho$  for both mother and calf, the milk ingestion rate function  $I_L$  (Table S1: eq. 7) evaluates to  
173  $9038/365 = \phi_L \cdot S^{2/3} \cdot 0.5$ . Using an average structural mass of the calf in the first year of  $S =$   
174  $\left( \int_0^{365} \omega_1 l(a)^{\omega_2} da \right) / 365 = 80.5 \text{ kg}$ , gives  $\phi_L = 2.7$ .

175 Parameters describing the efficiency of anabolic and catabolic reserve dynamics ( $\epsilon^+$  and  
176  $\epsilon^-$ ) were set to  $55 \text{ MJ} \cdot \text{kg}^{-1}$  and  $35 \text{ MJ} \cdot \text{kg}^{-1}$ , respectively. The efficiency of catabolism closely  
177 relates to the energy density of fat, which was reported as  $40 \text{ MJ} \cdot \text{kg}^{-1}$  (Lockyer 1993).  
178 Assuming a roughly 90% efficiency of catabolic conversion leads to the value of  $35 \text{ MJ} \cdot \text{kg}^{-1}$ .  
179 Anabolic conversion is considered less efficient and we hence set  $\epsilon^+$  to  $55 \text{ MJ} \cdot \text{kg}^{-1}$ .

180        The parameters  $\xi_c$  and  $\xi_m$  describe the non-linearity of milk assimilation with calf age and  
181      female body condition, respectively. Empirical estimates for these parameters do not exist for  
182      any marine mammal species. We therefore choose these parameters such that their functions  
183      reflect the biological response in a qualitative manner. The parameter  $\xi_m$  described how milk  
184      supply of the female depends on her body condition and is set to  $-2$ , to simulate a decline in the  
185      rate of milk provisioning that decreases with decreasing body condition of the female. The  
186      parameter  $\xi_c$  controls the steepness of the decrease in milk assimilation rate with increasing age  
187      of the calf. A value of  $\xi_c = 0.9$  ensures that milk suckling decreases with an increasing rate as  
188      the calf ages.

189        Mortality rate parameters are derived from Bloch et al. (1993a), who fit a survivorship  
190      curve to an age-frequency plot of Pilot Whales from the Faroe Islands ( $n = 1,482$  Bloch et al.  
191      1993a their Figure 3) and present age-specific survival estimates based on the method of Barlow  
192      and Boveng (1991). We use these age-specific survival estimates ( $P_a$ ) to calculate the age-  
193      specific mortality rate as  $z_a = -\ln(P_a)$ . Subsequently, we fit the mortality rate function in eq.  
194      (12) (Table S1) to the age-specific mortality rates  $z_a$  to obtain the estimates of the parameters  $\alpha_1$ ,  
195       $\alpha_2$ ,  $\beta_1$  and  $\beta_2$  as shown in Table S2. We set  $\mu_s$  to 0.2, which implies a starvation mortality rate  
196      of  $0.1 \text{ day}^{-1}$  for an individual with a body condition of 0.1 and (ignoring age-dependent  
197      mortality) a 50% survival over a period of one week of starvation if body condition remains at  
198      0.1.

199

- 200      *Literature Cited*
- 201      Barlow, J., and P. Boveng. 1991. Modeling Age-Specific Mortality for Marine Mammal  
202                Populations. *Marine Mammal Science* 7:50–65.
- 203      Bloch, D., C. Lockyer, and M. Zachariassen. 1993a. Age and Growth Parameters of the Long-  
204                Finned Pilot Whale off the Faroe Islands. Report of the International Whaling  
205                Commission, Special Issue 14:163–207.
- 206      Bloch, D., G. Desportes, R. Mouritsen, S. Skaaning, and E. Stefansson. 1993b. An Introduction  
207                to Studies of the Ecology and Status of the Long-finned Pilot Whale (*Globicephala melas*)  
208                off the Faroe Island, 1986 – 1988. Report of the International Whaling Commission,  
209                Special Issue 14:1–32.
- 210      Brody, S. 1968. Bioenergetics and Growth. Hafner Publishing Co., New York.
- 211      Kleiber, M. 1975. The fire of life: an introduction to animal energetics. R.E. Krieger Pub. Co.,  
212                Huntington, N.Y.
- 213      Kooijman, S. A. L. M. 2010. Dynamic Energy Budget theory for metabolic organisation. Third  
214                edition. Cambridge University Press, Cambridge, UK.
- 215      Lockyer, C. 1993. Seasonal Changes in Body Fat Condition of Northeast Atlantic Pilot Whales,  
216                and their Biological Significance. Report of the International Whaling Commission,  
217                Special Issue 14:325–350.
- 218      Martin, A. R., and P. Rothery. 1993. Reproductive Parameters of Female Long-Finned Pilot  
219                Whales (*Globicephala melas*) Around the Faroe Islands. Report of the International  
220                Whaling Commission, Special Issue 14:263–304.
- 221

**Table S1:** Model equations

Function	Equation	Description	Eq. no
$l_p(\tau_p)$	$l_b \frac{\tau_p}{T_P}, \quad 0 \leq \tau_p \leq T_P$	Length-age relationship of fetus	(1)
$l(a)$	$l_\infty - (l_\infty - l_b)e^{-ka}$	Von Bertalanffy growth in structural mass	(2)
$S(l)$	$\omega_1 l^{\omega_2}$	Structural mass-length relationship	(3)
$W(S, F, \tau_p)$	$\begin{cases} S + F + S(l_p(\tau_p)) & \text{pregnant} \\ S + F & \text{otherwise} \end{cases}$	Total mass of an individual	(4)
$W_M(S, F, \tau_p)$	$\begin{cases} S + \theta_F F + S(l_p(\tau_p)) & \text{pregnant} \\ S + \theta_F F & \text{otherwise} \end{cases}$	Maintenance mass of an individual	(5)
$I_R(a, R, S, F, W)$	$\phi_R R S^{2/3} \frac{1}{1 + e^{-\eta(\rho W/F-1)}} \frac{a^\gamma}{T_R^\gamma + a^\gamma}$	Energy assimilation rate from resource feeding	(6)
$I_L(a, S, F, W, F_m, W_m)$	$\phi_L S^{2/3} \frac{1}{1 + e^{-\eta(\rho W/F-1)}} \min\left(1, \left[ \frac{1 - \frac{a - T_N}{T_L - T_N}}{1 - \xi_c \frac{a - T_N}{T_L - T_N}} \right]_+ \right) \times \left[ \frac{(1 - \xi_m)(F_m - \rho_s W_m)}{(\rho - \rho_s)W_m - \xi_m(F_m - \rho_s W_m)} \right]_+$	Energy assimilation rate from milk	(7)
$C_M(W_M)$	$\sigma_M W_M^{3/4}$	Field metabolic costs	(8)
$C_G(l)$	$\sigma_G \omega_1 k (l_\infty - l) \omega_2 l^{\omega_2-1}$	Structural growth costs	(9)
$C_P(\tau_p)$	$\sigma_G \omega_1 \omega_2 \left( \frac{l_b}{T_P} \right)^{\omega_2} \tau_p^{\omega_2-1}, \quad 0 \leq \tau_p \leq T_P$	Pregnancy costs	(10)
$C_L(F, W, a_c, S_c, F_c, W_c)$	$I_L(a_c, S_c, F_c, W_c, F, W)/\sigma_L$	Lactation costs	(11)

---

$D(a)$	$\alpha_1 e^{-\beta_1 a} + \alpha_2 e^{\beta_2 a}$	Mortality rate	(12)
--------	--	----------------	------

$D_s(F, W)$	$\mu_s \left( \frac{\rho_s W}{F} - 1 \right), \quad F < \rho_s W$	Starvation mortality rate	(13)
-------------	---	---------------------------	------

$F_{neonate}$	$\frac{\sigma_G \omega_1 l_b^{\omega_2}}{\epsilon^-} + \frac{\rho_s \omega_1 l_b^{\omega_2}}{(1 - \rho_s)}$	Amount of reserve mass required to produce one neonate	(14)
---------------	---	--	------

	$F = \rho_s W + F_{neonate}$	Pregnancy threshold	(15)
--	------------------------------	---------------------	------

$R$	$\bar{R} \left( 1 + A \sin \left( \frac{2\pi t}{365} \right) \right)$	Resource dynamics	(16)
-----	---	-------------------	------

---

A '+'-subscript indicates that only positive values are used, *i.e.*  $f(x)_+ = \max(f(x), 0)$

**Table S2:** Model Parameters

Symbol	Unit	Value	Description	Source
$T_P$	day	365	Gestation period	Martin & Rothery 1993
$T_L$	day	1223	Lactation period (age at weaning)	Martin & Rothery 1993
$T_N$	day	365	Age at which milk consumption starts to decrease	–
$T_R$	day	500	Age at which resource foraging is 50%	–
$T_D$	day	445	Waiting period before onset of pregnancy	Martin & Rothery 1993
$l_b$	cm	177	Length at birth	Martin & Rothery 1993
$l_\infty$	cm	450	Ultimate length in Von Bertalanffy Growth Curve	Bloch et al. 1993; this study
$k$	day <sup>-1</sup>	0.00045	Von Bertalanffy growth rate	Bloch et al. 1993; this study
$\omega_1$	kg·cm <sup>-\omega_2</sup>	$8.5 \cdot 10^{-5}$	Structural mass-length scaling constant	Bloch et al. 1993; this study
$\omega_2$	–	2.6	Structural mass-length scaling exponent	Bloch et al. 1993; this study
$\theta_F$	–	0.2	Relative metabolic cost of reserves	–
$\rho$	–	0.30	Target body condition threshold	Lockyer 1993
$\rho_s$	–	0.15	Starvation body condition threshold	Lockyer 1993
$\phi_R$	$m^3 \cdot kg^{-2/3} \cdot day^{-1}$	1.0	Resource encounter rate scalar	–
$\phi_L$	$MJ \cdot kg^{-2/3} \cdot day^{-1}$	2.7	Lactation scalar	Lockyer 1993; this study
$\eta$	–	15	Steepness of assimilation response around target body condition	–
$\gamma$	–	2	Shape parameter of resource assimilation-age response	–
$\xi_m$	–	-2.0	Non-linearity in female body condition-milk provisioning relation	–

---

$\xi_c$	–	0.9	Non-linearity in milk assimilation-calve age relation	–
$\sigma_M$	$\text{MJ} \cdot \text{kg}^{-3/4} \cdot \text{day}^{-1}$	0.75	Field metabolic rate scalar	Lockyer 1993
$\sigma_G$	$\text{MJ} \cdot \text{kg}^{-1}$	30	Energetic costs per unit structural mass growth	this study
$\sigma_L$	–	0.86	Lactation conversion efficiency	Lockyer 1993
$\alpha_1$	$\text{day}^{-1}$	$4.01 \cdot 10^{-4}$	Mortality parameter	Bloch et al. 1993; this study
$\beta_1$	$\text{day}^{-1}$	$5.82 \cdot 10^{-4}$	Mortality parameter	Bloch et al. 1993; this study
$\alpha_2$	$\text{day}^{-1}$	$6.04 \cdot 10^{-6}$	Mortality parameter	Bloch et al. 1993; this study
$\beta_2$	$\text{day}^{-1}$	$3.01 \cdot 10^{-4}$	Mortality parameter	Bloch et al. 1993; this study
$\mu_s$	$\text{day}^{-1}$	0.2	Starvation mortality scalar	–
$\varepsilon^+$	$\text{MJ} \cdot \text{kg}^{-1}$	55	Anabolic reserves conversion efficiency	–
$\varepsilon^-$	$\text{MJ} \cdot \text{kg}^{-1}$	35	Catabolic reserves conversion efficiency	Lockyer 1993
$\bar{R}$	$\text{MJ} \cdot \text{m}^{-3}$	1.6 – 3.0	Mean annual resource density	–
$A$	–	0, 0.15, 0.3, 0.45	Relative amplitude of seasonal resource fluctuation	–

---

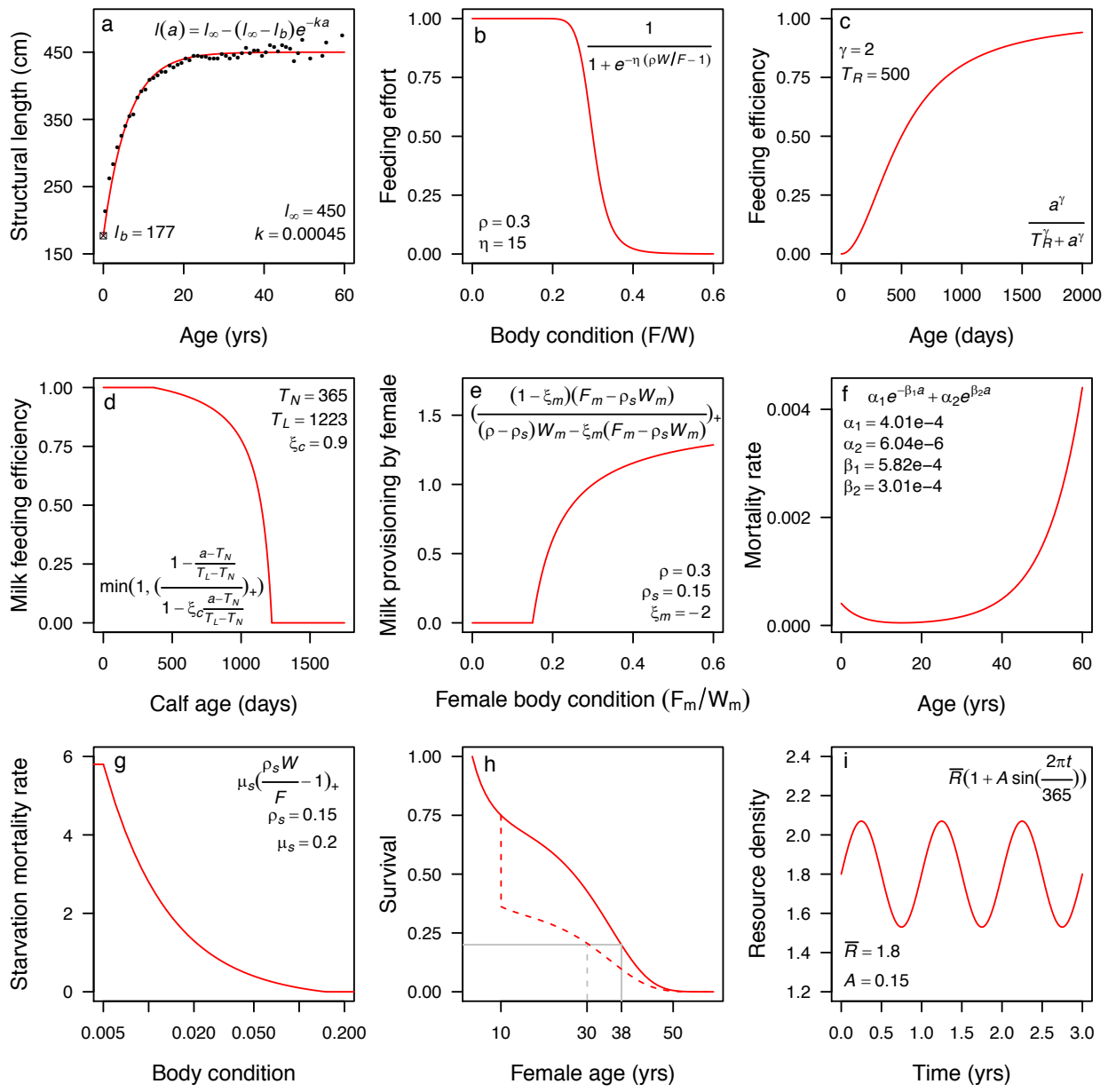


**Figure S1:** An overview of nine different model components and their associated functions and parameters. Some components are applied within the same model function. For example, panels b, d and e all appear in the function  $I_L(\dots)$ , that describes milk assimilation rate (eq. 7 in Table S1). The variables age  $a$  and time  $t$  are always in units of days, but for convenience sometimes plotted in years. Panel a shows data from Bloch et al. (1993a) on which the length-age relationship is parameterized with small solid points and the initial length at birth estimate as a

crossed open square. Panel h shows how mortality decreases survival for the female that is initiated at weaning age with a solid curve. Additionally, the dashed curve illustrates a particular scenario in which survival is affected by 15 days of starvation mortality at an age of 10 years. The gray lines in panel h indicate how starvation mortality reduces the life expectancy from 38 to 30 years. Subscript ‘+’ indicates positive values only, otherwise zero.

**Supporting Information.** Bio-energetic modeling of medium-sized cetaceans shows high sensitivity to disturbance in seasons of low resource supply  
*Vincent Hin, John Harwood & André M. de Roos.*

## Ecological Applications

### Appendix S2

**Figure S1:** Life history statistics as a function of disturbance period for both summer and winter disturbance and four different levels of resource seasonality (different columns). Each data point represents the mean of 1,000 life history simulations, each with a randomly determined life expectancy for both the female and each calf. Colors indicate bootstrapped 95% confidence intervals of the mean. LRO: lifetime reproductive output, Prop. weaned: proportion of calves that survive until weaning age, LE: life expectancy, AfR: age at first reproduction, AfW: female age at which first calf is weaned and IBI: inter-birth interval. The randomly determined life expectancy does not impose variation in age at first reproduction and for some data points at high disturbance values the lack of color bands indicates the coincidence of minimum and maximum values. Mean annual resource density  $\bar{R} = 2.0$  and all other parameters at default values (Appendix S1: Table S2).

